This is to certify that the
thesis entitled

A UNIQUE APPROACH TO FREQUENCY-MODULATED
CONTINUOUS-WAVE RADAR DESIGN

presented by

Gregory Louis Charvat

has been accepted towards fulfillment
of the requirements for the

Master of Science	degree in	Electrical Engineering

Major Professor's Signature

December 08, 2003

Date

A UNIQUE APPROACH TO FREQUENCY-MODULATED CONTINUOUS-WAVE RADAR DESIGN

By

Gregory Louis Charvat

A THESIS

Submitted to
Michigan State University
in partial fulfillment of the requirements
for the degree of

MASTER OF SCIENCE

Department of Electrical and Computer Engineering

2003

ABSTRACT

A UNIQUE APPROACH TO FREQUENCY-MODULATED CONTINUOUS-WAVE RADAR DESIGN

By

Gregory L. Charvat

Frequency-Modulated Continuous-Wave (FMCW) Radar has traditionally been used in short range applications. Conventional FMCW radar requires the use of expensive microwave mixers and low noise amplifiers. A uniquely inexpensive solution was created, using inexpensive Gunn oscillator based microwave transceiver modules that consist of 3 diodes inside of a resonant cavity. However these transceiver modules have stability problems which cause them to be unsuitable for use in precise FMCW radar applications, when just one module is used. In order to overcome this problem, a unique radar solution was developed which uses a combination of 2 transceiver modules to create a precise FMCW radar system. This unique solution to FMCW radar is proven to be capable of determining range to target, and creating Synthetic Aperture Radar images.

This Masters Thesis is dedicated to those individuals who continue to be a positive influence in my life, and have always encouraged my work:

Dave and Rita Charvat

Louis and Jane Charvat

Gerard and Therese Nefcy

"Look, Gail." Roark got up, reached out, tore a thick branch off a tree, held it in both hands, one fist closed at each end; then, his wrists and knuckles tensed against the resistance, he bent the branch slowly into an arc. "Now I can make whatever I want of it: a bow, a spear, a cane, a railing. That's the meaning of life."

Ayn Rand, "The Fountainhead"

TABLE OF CONTENTS

LIST OF TABLES

LIST OF FIGURES

Chapter 1

Overview

Continuous-wave (CW) radar is an old concept. CW radar uses a simple coherent design topology. When frequency modulated (FM), CW radar can be used as a precise short range radar. CW radar has been in widespread use since the mid 1930's. CW radar is advantageous for use in precision Doppler measurements. A great variety of microwave parts are available for use in CW radar systems. A unique solution to CW radar was created using a pair of inexpensive Gunn diode based microwave transceivers. Test results on this unique solution were positive, proving that it was capable of short range to target measurements, and a viable solution for use in a Synthetic Aperture Radar (SAR) system.

CW radar is based on a coherent radar design topology. The fundamental difference between a simple coherent radar (see figure 1.1) and a CW radar (see figure 1.2) is the absence of a transmit mixer. In a CW radar, the transmit oscillator is connected directly to the transmit antenna. Some of the transmit oscillator's power is coupled off and used to feed a receive mixer. A second antenna is connected to the input of that mixer. The mixer beats in the difference between the transmit oscillator and any RF received in the RF input port. The IF output of the mixer is the Doppler shift reflected from a moving target. When this system is FM modulated, the radar can precisely indicate range to

target as a function of frequency. This type of radar is known as FMCW. The time difference between the FM modulated carrier being transmitted and the carrier that is reflected off of a target can be measured on the IF output port of the receive mixer. This time difference is in the form of frequency, and can be counted or analyzed as a function of distance to target.

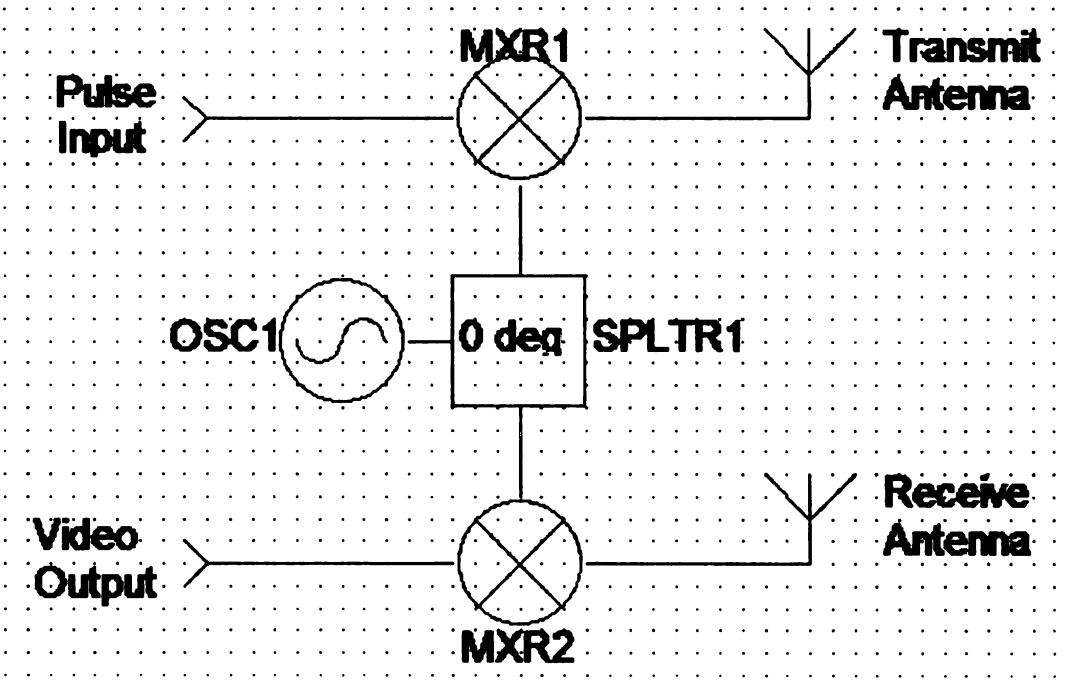

Figure 1.1: Simplified coherent radar block diagram.

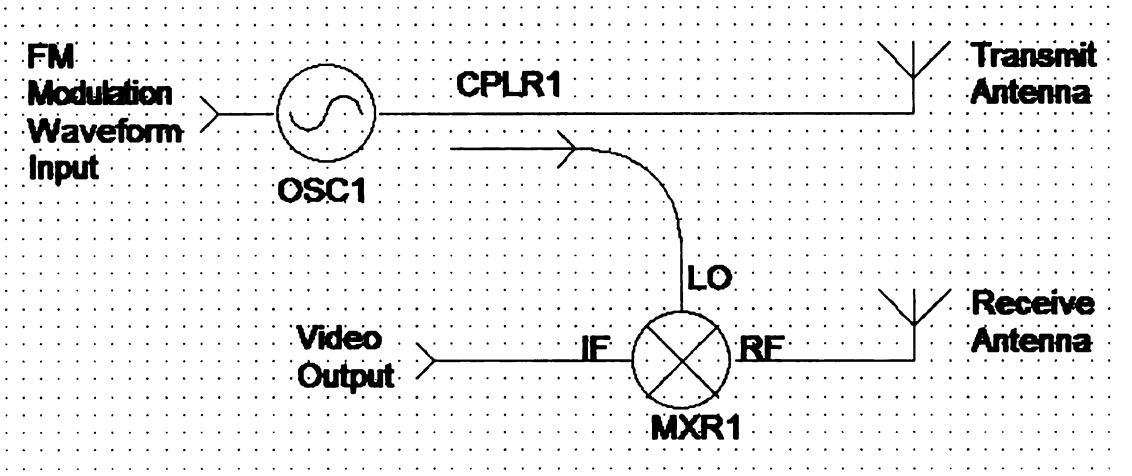

Figure 1.2: Simplified CW radar block diagram.

Wide spread use of FMCW radar first occurred during the mid 1930's [3]. Radio altimeters mounted on aircraft made use of FMCW radar to measure the distance from the aircraft to the ground directly below. Early radio altimeters used mechanical methods to create the FM chirp needed to acquire range information. A typical design would include an electric motor attached to an air variable capacitor used to modulate the frequency of the transmit oscillator. The FM modulated transmission would allow range data to be extracted from the return echo off of the ground below.

Many inexpensive microwave components and assemblies are currently available to designers. One of the most inexpensive microwave components available today is a transceiver module based around a Gunn oscillator with a varactor tuning diode, and a Schottky mixer diode. This inexpensive microwave transceiver is widely known as the Gunnplexer. A unique approach to FMCW radar was designed using the inexpensive transceiver modules. This design incorporates two transceiver modules in a bistatic

configuration, where RF power from one is leaked into the other, creating a self tracking coherent FMCW radar system.

Test results were positive. The unique solution to FMCW radar was proven effective in measuring range to target. The unique radar solution was then successfully used to create a SAR imaging system. This research has concluded that using two inexpensive microwave transceiver modules in unison can yield extremely good performance for use as an FMCW radar system at a low cost. This research has also concluded that the unique solution to FMCW radar is capable of performing in the most advanced applications, such as Synthetic Aperture Radar.

Chapter 2

General Theory of Operation

Two types of CW radar will be examined here. An introduction to Synthetic Aperture Radar theory will also be presented. The first type of CW radar is the unmodulated CW Doppler radar system. The second type of CW radar is the frequency modulated FMCW radar system. CW radar systems have been proven useful in measuring precision Doppler shifts on moving targets. FMCW radar systems have been proven useful in measuring both Doppler shifts of moving targets and range to moving or fixed targets. CW radar is often a simple cost effective solution to Doppler and short range measurements. One useful application of CW radar is Synthetic Aperture Radar.

2.1 Unmodulated CW Doppler Radar System

Unmodulated CW radar is frequently used to precisely measure Doppler shifts of moving targets. The block diagram of a simple CW radar system is shown in figure 2.1.

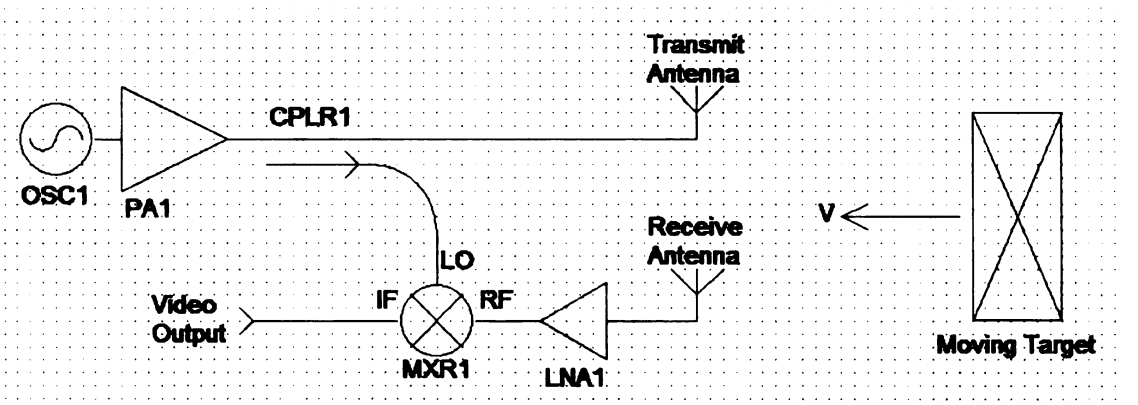

Figure 2.1: Block diagram of a CW Doppler radar system.

Looking at figure 2.1, the fixed oscillator OSC1 drives the power amplifier PA1. The output carrier wave from PA1 is fed to the transmit antenna, and radiated out to the moving target. The carrier reflected off the moving target is Doppler shifted by a frequency of f_d Hz given by the equation [1]:

$$f_d = \frac{2v_r f_r}{c} \tag{2.1}$$

Where: f_r = transmitted frequency (Hz)

c = velocity of propagation (m/sec)

v_r = relative velocity of the moving target to the radar (m/sec)

The reflected signal from the target is amplified by LNA1. The output of LNA1 is fed into the RF port of MXR1. Some power from the output of PA1 is coupled into the local oscillator (LO) port of mixer MXR1. The product of the reflected signal from the target and the carrier output of PA1 are acquired from the IF port of MXR1. Thus IF port output of MXR1 is the Doppler shift f_d due to the moving target. This is shown by equations 2.2 through 2.4.

Frequency reflected from the moving target:

$$f_{reflected} = f_{OSC1} + f_d \tag{2.2}$$

Frequency output of the IF port of MXR1 (neglecting the high frequency mixer product because of the high frequency cut-off of most practical microwave mixers):

$$f_{IF} = f_{reflected} - f_{OSC1} \tag{2.3}$$

And it is proven, the frequency at the IF port of MXR1:

$$f_{IF} = f_d \tag{2.4}$$

The amplitude of signal reflected from the moving target is a function of the radar range equation:

$$\begin{aligned} P_{r(dB)} &= P_{t(dB)} + G_{t(dB)} + G_{r(dB)} + \sigma_{(dB)} - 20\log(f_{OSC1}) - \\ &- 40\log(R) - 30\log(4\pi) + 20\log(c) \end{aligned} \tag{2.5}$$

Where: $P_{r(dB)}$ = relative logarithmic power collected by the receive antenna in dB

$P_{t(dB)}$ = relative logarithmic power transmitted by the transmitter in dB

$G_{t(dB)}$ = logarithmic gain of the transmit antenna in dB

$G_{r(dB)}$ = logarithmic gain of the receive antenna in dB

σ_{dB} = radar cross section (RCS) of the moving target in dBsm

R = range to target in meters

The basic principles of CW Doppler radar are not difficult to understand. The CW Doppler radar system described here can be constructed easily with coaxial parts from manufacturers such as Mini-Circuits and Miteq. A radar system such as this is very effective in performing Doppler measurements.

2.2 Frequency Modulated Radar

When modulated, a CW radar system is capable of providing range to target information. When a CW radar system is FM modulated, the range to target information provided is in the form of beat frequencies. This is known as FMCW radar. The beat frequencies on the video output of an FMCW radar system correspond to multiple targets and their ranges. FMCW radar systems are also capable of measuring the Doppler shift of a moving target. The block diagram of a basic FMCW radar system is shown in figure 2.2.

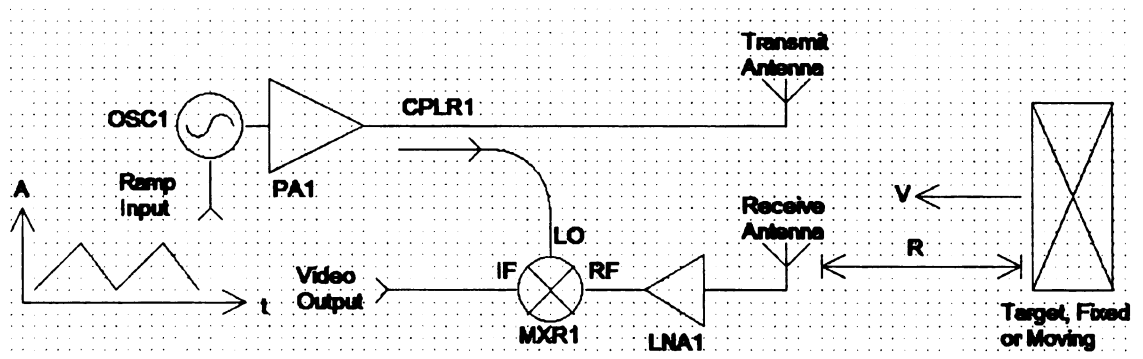

Figure 2.2: Block diagram of a basic FMCW radar system.

Looking at figure 2.2, OSC1 is FM modulated with a triangular ramp input with a period of 2 ms. The triangular ramp is an alternating linear ramp with both positive and negative slopes as shown in figure 2.3.

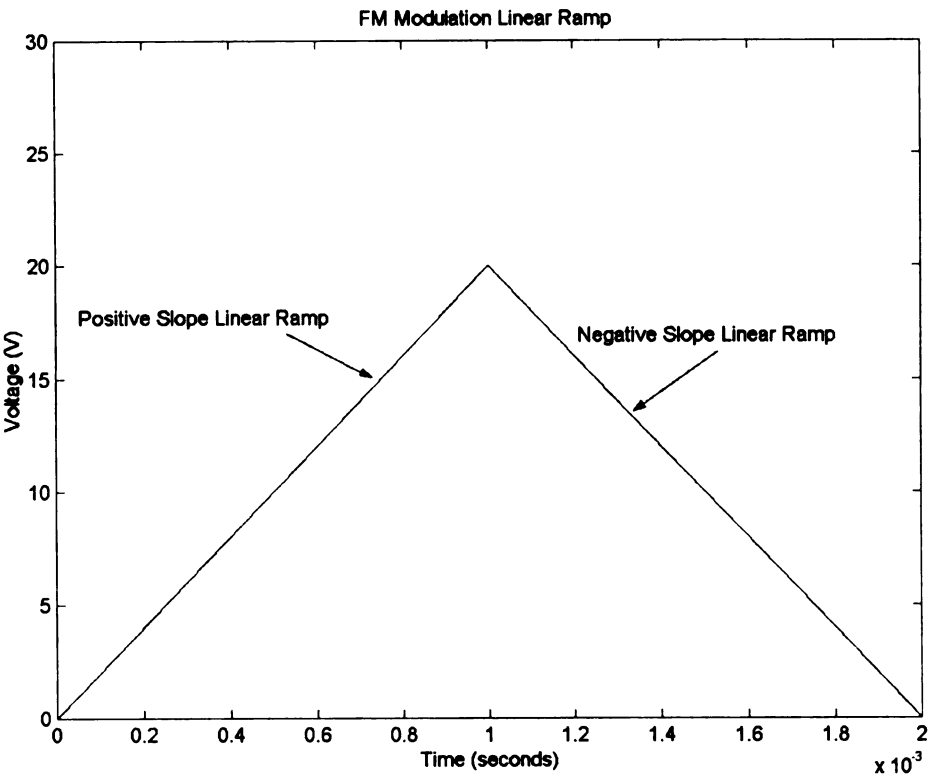

Figure 2.3: Linear ramp used to FM modulate the FMCW radar system.

The FM output of OSC1 is fed into PA1. PA1 amplifies OSC1 to an appropriate transmit level. The output of OSC1 is radiated out of the transmit antenna. The FM modulated carrier is reflected off of the target at a range of R meters. The reflected signal is delayed in time on its way to and from the target. The reflected signal is received by the receive antenna, and amplified by LNA1. The output of LNA1 is fed into the RF port of MXR1. Some power from PA1 is coupled into the LO port of MXR1. When the LO and the RF are multiplied together in MXR1, the IF output of MXR1 is the range to target in frequency. This range to target in terms of frequency is known as the beat frequency. The greater the beat frequency on the IF output port of MXR1, the greater the range to

target. If the target is moving, then the Doppler shift of the moving target is added onto the beat frequency present on the IF port of MXR1. The relationship between frequency, FM chirp bandwidth, range to target, and Doppler frequency shift can be found using the equations for both a positive and a negative linear ramp modulation waveform [2]. When a positively sloped linear ramp FM modulates OSC1, the beat frequency at the IF port of MXR1 is represented by:

$$f_b = f_b^+ = \frac{8\Delta f f_m R}{c} - f_d \tag{2.6}$$

Where: f_b = the beat frequency at the IF port of MXR1

f_b^+ = the beat frequency at the IF port of MXR1 when OSC1 is modulated with a positive linear ramp.

Δf = chirp frequency deviation

f_m = FM modulation rate

R = range to target

When a negatively sloped linear ramp FM modulates OSC1, the beat frequency at the IF port of MXR1 is represented by:

$$f_b = f_b^- = \frac{8\Delta f f_m R}{c} + f_d \tag{2.7}$$

Where: f_b^- = the beat frequency at the IF port of MXR1 when OSC1 is modulated with a negative linear ramp

From the equations above, the range to target is found using:

$$R = \frac{c}{8\Delta f f_m}\langle f_b \rangle \tag{2.8}$$

Where: $\langle f_b \rangle$ = the average frequency difference

If the target is moving, the velocity of the target can be found using:

$$v = \frac{\lambda}{4}\left(f_b^- - f_b^+\right) \tag{2.9}$$

The amplitude of the return signals can be approximated using the logarithmic radar range equation 2.5.

The basic principle of FMCW radar is somewhat difficult to conceptualize. The most important concept explained here is that a shift in time corresponds to a shift in frequency. This is because the radar is frequency modulated in time. The current value of the transmitted frequency is different than what was transmitted 2 ns ago. These small and subtle frequency differences make up the beat frequencies on the IF output of MXR1, and hence the range to target information in the form of low frequency beats.

FMCW radar systems are capable of measuring distances of very close targets with high accuracy. The range resolution obtainable by an FMCW radar system depends on its transmitted chirp bandwidth. The more frequency that is covered during a chirp, the higher the range resolution. It is also important to transmit an extremely linear frequency chirp. Any nonlinearities in the frequency chirp reduces range resolution and maximum unambiguous range.

The maximum range resolution obtainable for an FMCW radar system depends on the chirp bandwidth:

$$B = 2\Delta f \tag{2.10}$$

Where: B = chirp bandwidth

The maximum range resolution is determined using the equation:

$$\delta R = \frac{c}{2B} \tag{2.11}$$

Where: δR = maximum range resolution

The maximum range resolution only occurs when round trip time for the signal, T, is substantially less than the time it takes for one full chirp:

$$T = \frac{2R}{c} << \frac{1}{f_m} \tag{2.12}$$

Where: T = round trip time for the radar signal to reach its target and be reflected back to the radar

The maximum range at which the radar can detect and accurately measure range is known as the maximum unambiguous range. The maximum unambiguous range can be determined using the following equation:

$$R_m = \frac{c}{2f_m} \tag{2.13}$$

Where: R_m = the maximum unambiguous range

FM tuning linearity is extremely important to characterizing both range resolution and maximum unambiguous range. Both are adversely affected by poor FM chirp linearity. The FM chirp linearity accuracy required when given a desired range resolution and maximum unambiguous range can be determined using the equation:

$$\frac{\delta f}{B} = \frac{\delta R}{R_m} = \text{chirp nonlinearity} \tag{2.14}$$

Where: δf = deviation of chirp from linear

An example of determining the required chirp nonlinearity for a desired range resolution and maximum unambiguous range:

> An FMCW radar system is required to have a range resolution of 2 feet, and a maximum unambiguous range of 150 feet. Thus, the chirp must not be any more than 1.33% nonlinear.

2.3 Synthetic Aperture Radar (SAR)

An FMCW radar system can be used as the radar unit in a Synthetic Aperture Radar system. A SAR system is capable of creating detailed radar images. These images are created by combining range profiles from the FMCW radar unit at many different locations. A range profile is defined as the range to target information acquired from a radar system. When a number of individual range profiles are combined together in a certain way through a SAR process, it is possible to create a detailed radar image.

For this application, a focused array SAR system will be explored [6]. In a focused array SAR system, a large number of range profiles are collected and spaced at a defined interval. The large number of range profiles are collected by moving the radar in a straight line, and projecting the antenna beams outwards in a perpendicular direction to that line, as shown in figure 2.4.

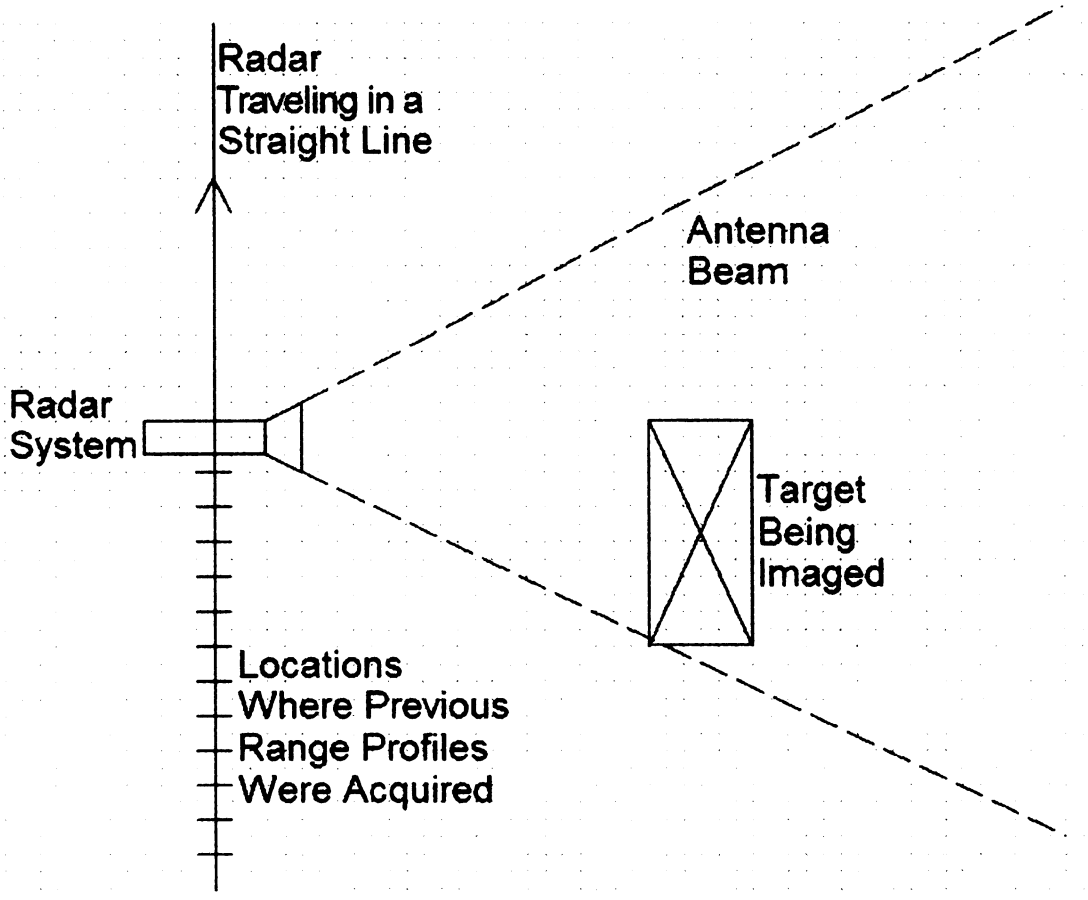

Figure 2.4: Range profiles acquired in a straight line, where the antenna beam of the radar system is perpendicular to the line.

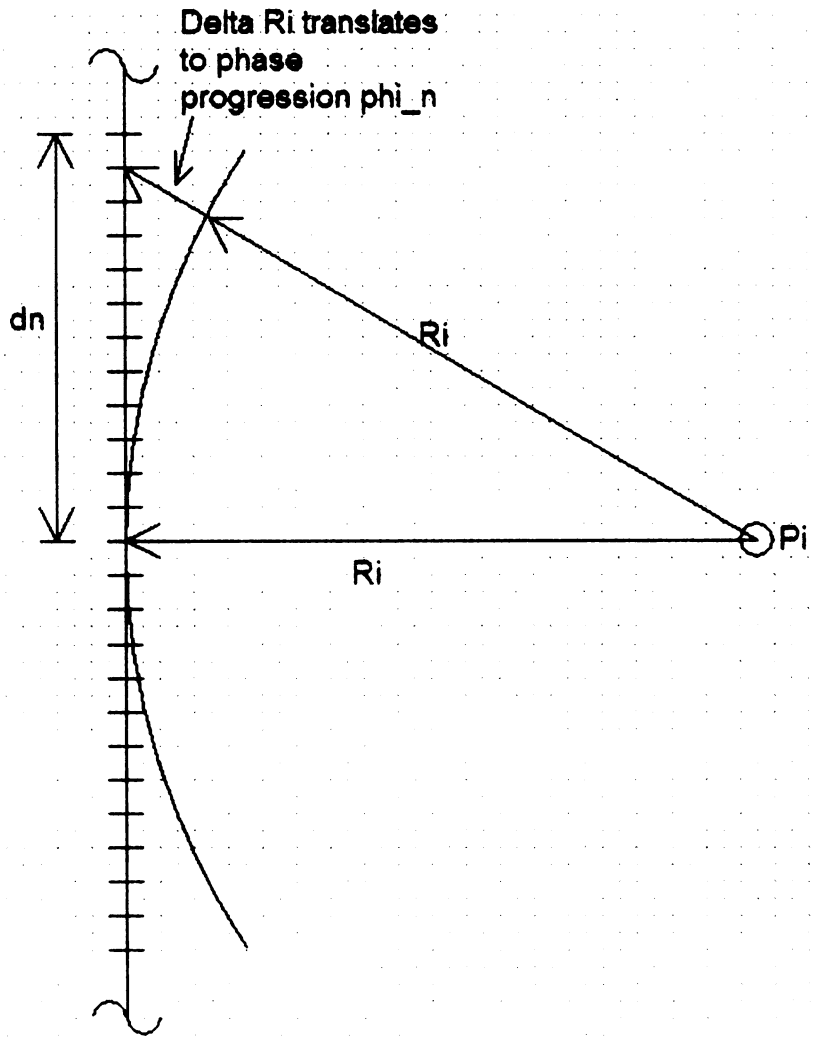

Figure 2.5: Phase error progression of an n-element synthesized aperture.

Of all the range profiles acquired, every N number of range profiles collected are used to synthesize an N element focused array. The array of N elements is focused onto each point P_i at a range R_i downrange from the radar and centered in the middle of the array (see figure 2.5). When the aperture is looking at the point P_i, a progressive phase error occurs between the center of the array and each element on either side of the center of the

array, as shown in figure 2.5. This progressive phase error is approximated using the equation:

$$\phi_n \cong \frac{2\pi}{\lambda}\left(\frac{d_n^2}{R_i}\right) \text{ radians} \tag{2.15}$$

Where: ϕ_n = phase error

d_n = distance from center of N element array

n = n'th element from the center of the N element array

R_i = range to point P_i

The N element array is then focused on to point P_i at range R_i using the phase error equation 2.15. This focusing procedure is achieved by using the following equations:

$$x_n^{'} = x_n \cos\phi_n + y_n \sin\phi_n \tag{2.16}$$

Where: $x_n^{'}$ = the phase compensated real component of the n'th element in the N element array

x_n = the uncompensated real component of the n'th element in the N element array

y_n = the uncompensated imaginary component of the n'th element in the N element array

$$y_n^{'} = y_n \cos\phi_n - x_n \sin\phi_n \tag{2.17}$$

Where: $y_n^{'}$ = the phase compensated imaginary component of the n'th element in the N element array

The sum of the real and imaginary components of the phase compensated N element array are then summed:

$$X = \sum_{n=1}^{N} x_n^{'} \tag{2.18}$$

Where: X = the sum of all the phase compensated real components of the N element array

N = N element array length

$$Y = \sum_{n=1}^{N} y_n^{'} \tag{2.19}$$

Where: Y = the sum of all the phase compensated imaginary components of N element array

The magnitude of the sum of real and imaginary components of the N element array is taken using the equation:

$$S = \sqrt{X^2 + Y^2} \tag{2.20}$$

Where: S = the magnitude of the focused N element array on point P_i at range R_i

This magnitude is then saved as a new range bin which represents the distance R_i. The entire process is repeated again for range R_{i+1}, where the resulting magnitude is stored as a new range bin which represents the distance R_{i+1}. The process is repeated until the N element array has produced a focused magnitude for every single range bin.

After the N element array is finished focusing on every range bin, it moves on. The radar is moved forward by one increment and a range profile is acquired. The new range profile, plus the previous N-1 range profiles are used to synthesize and focus another N element array, where the procedure described above is performed again.

This entire process is performed repeatedly, producing lines of focused range bins, until the user of the radar system decides to stop. The resulting focused range bins and their accompanying focused magnitudes are then used to construct a detailed Synthetic Aperture Radar image.

Summary:

FMCW radar is a proven technology capable of precisely ranging targets at close ranges. It is also capable of measuring the Doppler shift of a moving target. The basic FMCW radar system description and accompanying equations described above are extremely important to understanding the concept and some design aspects of this type of radar system. An FMCW radar system also has the potential to be used as a Synthetic Aperture Radar. The principles of SAR explained in this section are essential to understanding the application of FMCW in a SAR system.

Chapter 3

Practical FMCW Radar Systems, Past and Present

FMCW radar has been in use for many years. Its widespread use first started in the mid 1930's, where it was used in aircraft radio altimeters. There were many design challenges in implementing early FMCW radar systems. Those challenges included generating a linear chirp, acquiring frequency domain range data, and antenna coupling issues. Many of the design issues of early FMCW systems are still a challenge today. These include antenna coupling, and creating a precision chirp using an inexpensive oscillator. Regardless of the design challenges of FMCW radar, it has proven an effective way to measure range and Doppler shift in many applications.

FMCW radar was first used primarily in aircraft radio altimeters. The radio altimeter used FMCW radar to measure the distance from the aircraft to the ground below (see figure 3.1). Unlike a conventional altimeter, which indicates altitude above sea level, the radio altimeter indicates altitude above anything on ground, including mountains, trees, and other terrain features. One example of an early radio altimeter was the Western

Electric Type 1A radio altimeter [3]. The Type 1A was introduced in 1936. It had a maximum height range of roughly 5000 feet.

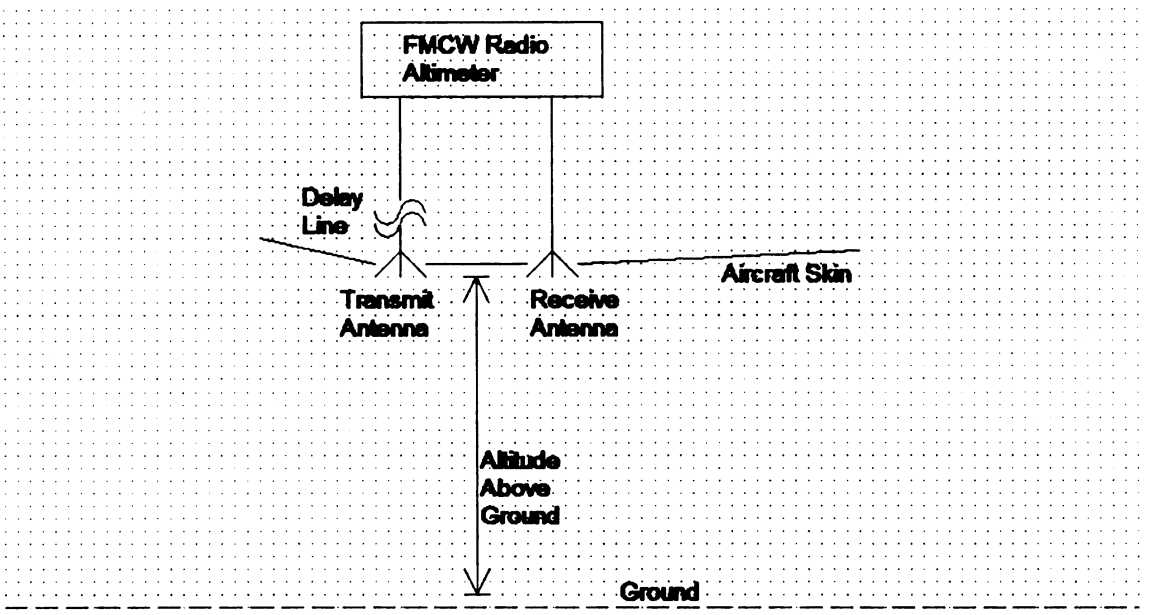

Figure 3.1: Radio altimeter installed on an aircraft.

Early radio altimeters used mechanical methods to generate a linear frequency chirp. Typical mechanical frequency modulation methods included agitating or moving crucial parts of a VHF or microwave oscillator. These parts that were mechanically agitated were usually made of a non-conducting dielectric inside of a microwave cavity oscillator, or an air variable cap. An example of early radio altimeter modulation schemes is the Raytheon model AN/APN-22 [4]. Developed for the US Navy in 1954, this radio altimeter used a CW cavity magnetron transmitting tube which was feeding a horn antenna, connected together using waveguide. The magnetron would chirp from 4.2 GHz to 4.4 GHz using a mechanical vibrating reed system. The vibrating reed varied the

capacitance across the straps of the anode cavity on the magnetron assembly. This vibrating reed was controlled by a magnetic coil, similar to that of a loudspeaker. A second coil was also connected to the reed, allowing for feedback control of the vibrating reed.

One of the more interesting methods of producing a chirp is in using a rotating air variable capacitor [5]. A small electric motor would be connected to an air variable capacitor, which would rotate, producing FM modulation in the transmitter oscillator circuit (see figure 3.2).

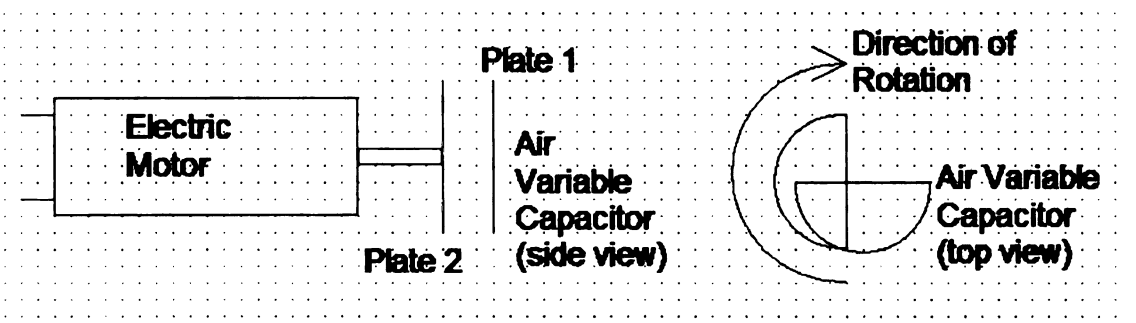

Figure 3.2: Rotating air variable capacitor chirp mechanism.

Modern FMCW radar systems typically use a solid state varactor diode to modulate the frequency of the transmit oscillator. The varactor diode is typically placed in the resonant tank circuit of a free-running oscillator. With the varactor diode placed in the tank circuit, the free-running oscillator becomes a voltage controlled oscillator (VCO). Varactor diodes are not the most linear way of shifting the frequency of a VCO, however they are the least expensive solid state solution to creating an FM chirp. Great care must be taken in determining the most linear range of operation of a varactor tuned VCO when

used as the transmit oscillator of an FMCW radar system. The Bendix ALA-51A is an example of radio altimeter that uses a varactor diode to modulate its transmit oscillator [1]. The yttrium-iron-garnet (YIG) oscillator is a good alternative to the varactor VCO. A YIG oscillator is a ferromagnetic tunable resonator, in which the frequency is varied by changing a DC current controlling a magnetic field, for this reason YIG oscillators have excellent tuning linearity. YIG oscillators can be used as VCO's, and will produce a low distortion linear chirp, ideal for FMCW radar. Because of their excellent tuning linearity linearity, YIG oscillators are often used as the sweep LO in most modern spectrum analyzers and network analyzers. However you will not find them in most FMCW radio altimeters because YIG oscillators are very expensive, and are not suitable for a cost effective FMCW radar solution.

Acquiring and processing range data from an FMCW radar system has always been a challenge. Early, and many current, FMCW radar systems use a simple frequency counter. There is a difference, however, between early and modern frequency counters. The early counters would use a frequency to voltage converter of some type [4] [5], and display the range data on an analog meter display. Modern radio altimeters, such as the Bendix ALA-51A, use a conventional digital frequency counter. Both early and modern radio altimeters use an interesting trick in the video signal chain to scale the return amplitudes of high and low altitudes. Low altitudes beat in as relatively low audio range frequencies. High altitudes beat in as relatively high audio range and low RF range frequencies. The amplitude return from the ground of a low altitude beat is much higher than that of a high altitude beat. Thus, the designers of radio altimeters use a high pass

filter in the video chain to attenuate the low altitude beat signals, and amplify the high altitude beat signals [1]. This high pass filter typically has a cut off response of 6 dB per octave. It is placed in series with the video signal chain, before the frequency counter as seen in figure 3.3. The output of the high pass filter is fed into a limiting amplifier. That amplifier is fed into a frequency counter which counts 0 V crossings. The output of the frequency counter is fed into an altitude display indicator.

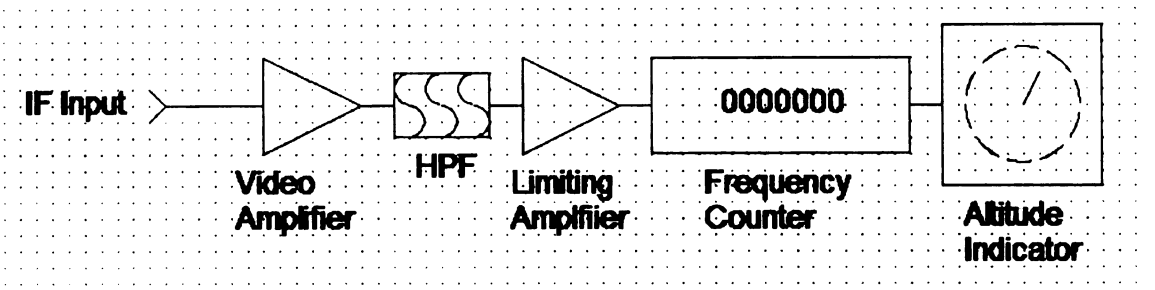

Figure 3.3: Typical method for scaling altitude return signal level, processing return distance, and displaying altitude used in radio altimeters.

FMCW radar range data can also be processed by digitizing the video output. Multiple target returns can be acquired by processing the digitized video output of an FMCW radar system. This is achieved by performing a Fast Fourier Transform on the digitized waveform (see figure 3.4). The resulting frequency plot indicates the target ranges in terms of frequency, and target return amplitudes. With modern digitizer technology, it is possible to expand the applications for FMCW radar systems, beyond simple range to large target applications.

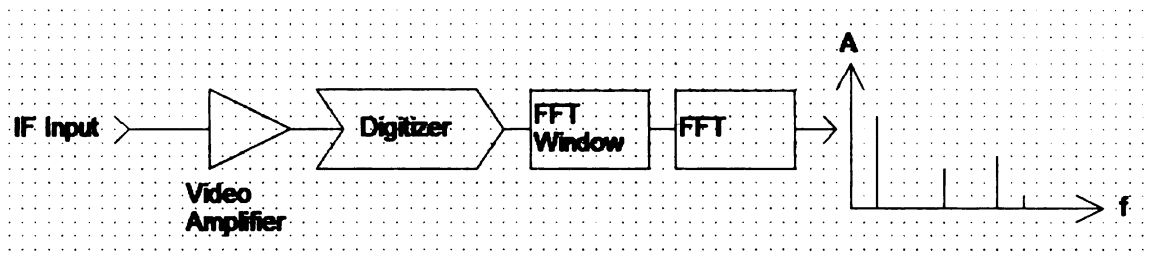

Figure 3.4: The video output of an FMCW radar system can be digitized, and with some simple signal processing, the range to target data displayed in the frequency domain.

Antenna coupling is the one problem that has always plagued FMCW radar designers since the 1930's to present day. Antenna coupling limits the sensitivity of the receiver, and the dynamic range of the entire radar system [1]. Coupling can be measured from the transmit antenna to the receive antenna by measuring the power at the receive antenna that is picked up by the transmitter as shown in figure 3.5.

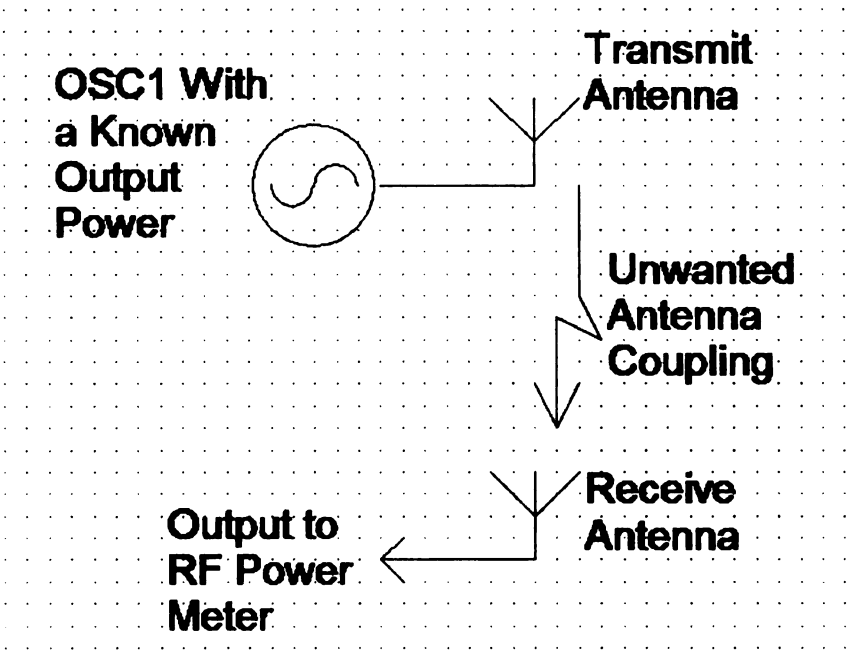

Figure 3.5: Antenna coupling limits the sensitivity and dynamic range of FMCW radar systems.

The problem of antenna coupling can be uniquely solved in FMCW radar systems. The coupling produces a beat frequency in the video chain of the radar system. This beat frequency corresponds to the delay between the transmitter to transmit antenna, through the coupling path, and through the receive antenna back to the receiver. This delay and its corresponding beat frequency can be nullified by inserting a delay line between the transmitter and transmit antenna, or the receiver and receive antenna. An example of this is shown in figure 3.1. This method nullifies the beat frequency seen in the video signal chain caused by the antenna coupling. However, this method cannot solve problems such as saturation in the receiver front end due to too much power coupled from the

transmitter at the receive antenna. Problems such as these are best solved with better antenna arrangements, and decoupling techniques.

Delay lines have the potential to cause problems. Modern radio altimeters and other FMCW radar systems operate at high microwave frequencies, such as the Bendix ALA-51A. Delay lines are typically waveguides or microwave coax cables. When a delay line is inserted before the LNA in a receiver, it introduces losses which add directly to the noise floor of the receiver. This increased noise floor causes a further reduction in sensitivity and dynamic range. Careful consideration must be used in the placement of delay lines.

Summary:

FMCW radar systems have been in use since the mid 1930's. Modern FMCW radar systems are much different, and also very similar in many ways to the early models. FMCW radar continues to be primarily used in the application of radio altimeters. But with modern data acquisition and signal processing methods, FMCW radar systems show potential for other applications.

Chapter 4

Theory of Operation

A unique FMCW radar system was designed by the author utilizing inexpensive, readily available microwave transceiver modules. This system is based around a pair of M/A-Com MA87127-1 X-band microwave transceiver modules. These modules are configured in an unusual way such that a deliberate coupling is created between the transmit and receive horn antennas. This deliberate coupling facilitates a unique approach to FMCW radar.

4.1 The MA87127-1 Gunn Diode Based Transceiver Module

The MA87127-1 transceiver module is an inexpensive X-band microwave transceiver solution. It is small and compact, as shown in figure 4.1.

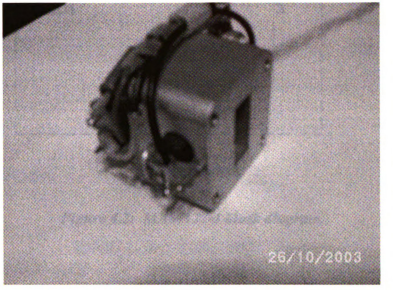

Figure 4.1: The MA87127-1 microwave transceiver module.

The MA87127-1 is composed of three major components, VCO, mixer, and circulator as shown in figure 4.2. The VCO is fed into port 1 of the circulator. Port 2 of the circulator is connected to the WR-90 waveguide flange input/output port of the transceiver. Port 3 of the circulator is connected to the RF input of the mixer. Some power is coupled off the VCO and fed into the LO port of the mixer. The IF output of the mixer is connected to a small solder terminal on the outer case of the transceiver.

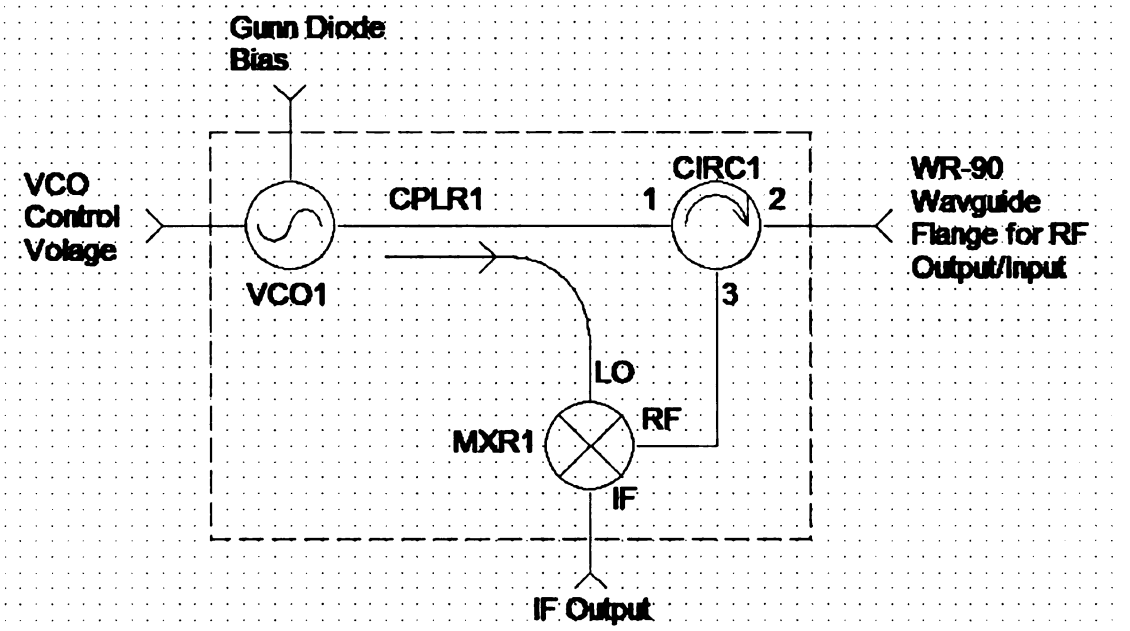

Figure 4.2: MA87127-1 block diagram.

VCO1 is a varactor controlled Gunn diode oscillator. A varactor diode is placed inside of a cavity Gunn oscillator as shown in figure 4.3. A bias voltage on the varactor diode between, roughly, 0 and 20 V controls the frequency of the Gunn oscillator. A second bias voltage of approximately 10 V is needed to cause the Gunn diode to oscillate at the frequency of the cavity that it is placed in.

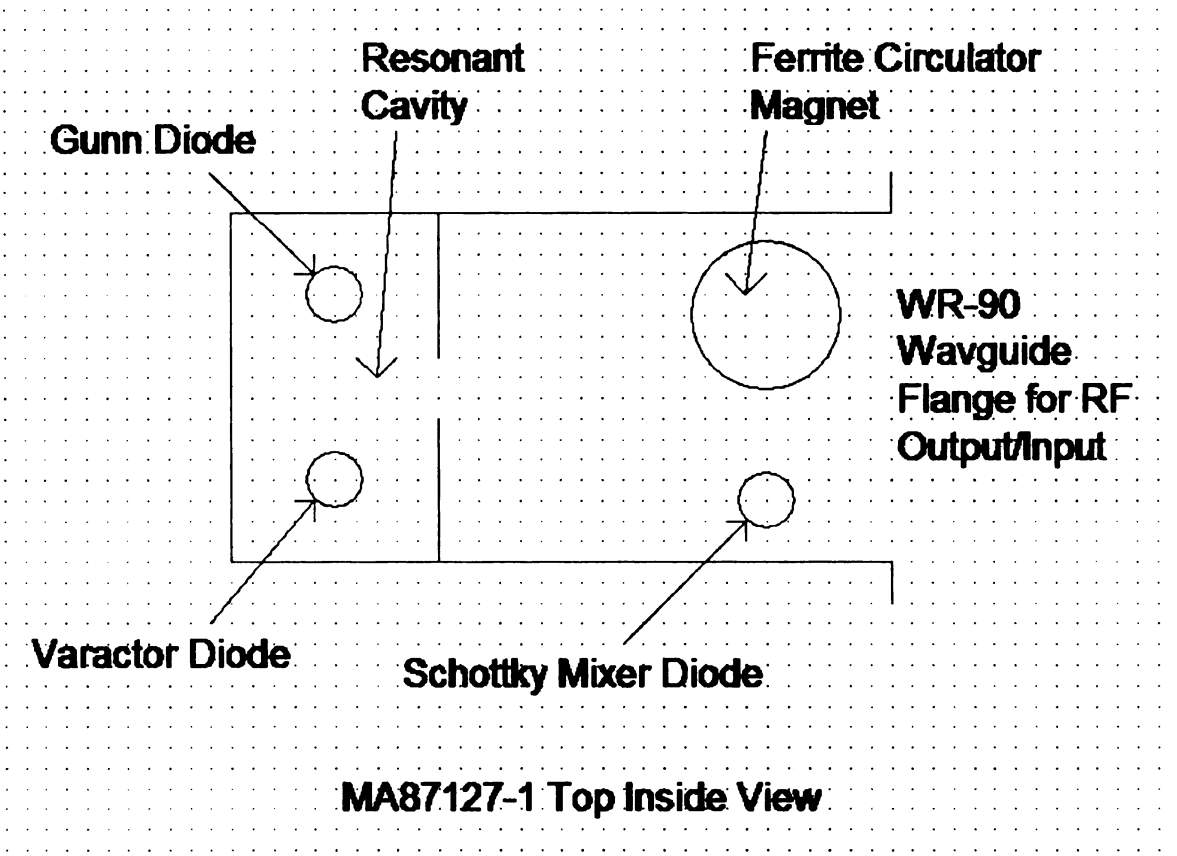

Figure 4.3: MA87127-1 Physical Layout.

CPLR1 is a symbolic representation of the coupling action that occurs between the Gunn oscillator diode and the Schottky mixer diode placed within close proximity (see figure 4.3). The close proximity of the Schottky mixer diode to the Gunn diode causes a coupling to occur.

MXR1 is created by the coupled power from CPLR1. The coupled power from the Gunn diode oscillator causes the Schottky mixer diode to switch on and off. This switching action causes the Schottky mixer diode to operate as a single balanced mixer.

CIRC1 is a ferrite circulator place inside of the resonant waveguide cavity that contains VCO1 and MXR1. CIRC1 is basically a large magnet precisely placed inside of the resonant cavity. CIRC1 causes RF power from VCO1 to exit the input/output port, and causes RF power coming into the input/output port to be transferred into MXR1.

When looking at figure 4.2, it appears as though one transceiver module alone can be utilized as an FMCW radar system. However, it was found in lab tests that the pass band of the IF port on MXR1 starts to roll off around 1 MHz, causing little to no response at audio frequency, which is were most beats from a short range FMCW radar system will be located. The transceiver module's receiver worked most efficiently above 30 MHz, where the loss due to the mixer was found to be the least. The lack of an acceptable low frequency to DC response from MXR1 renders one individual transceiver module useless for short range FMCW radar use. This problem is common for most microwave transceiver modules of this type.

Another problem often encountered with this type of transceiver module is frequency drift. According to the specifications, the MA87127-1 will drift at a rate of 350 KHz per 1 degree Celsius. It was also found in lab tests that the transceiver module drifts off frequency when it encounters sever VSWR reflections on its input/output port.

The tuning linearity of the varactor diode controlled Gunn oscillator is not very good. For practical uses, a linear tuning range must be found by experimentation after the transceiver module is installed into whatever system it might be used in.

4.2 A Unique FMCW Radar Solution

The MA87127-1 X-band microwave transceiver module is not capable of accurate FMCW radar operation by itself. However, when two MA87127-1 (or similar) transceiver modules are used, the unique FMCW radar design solution can be obtained.

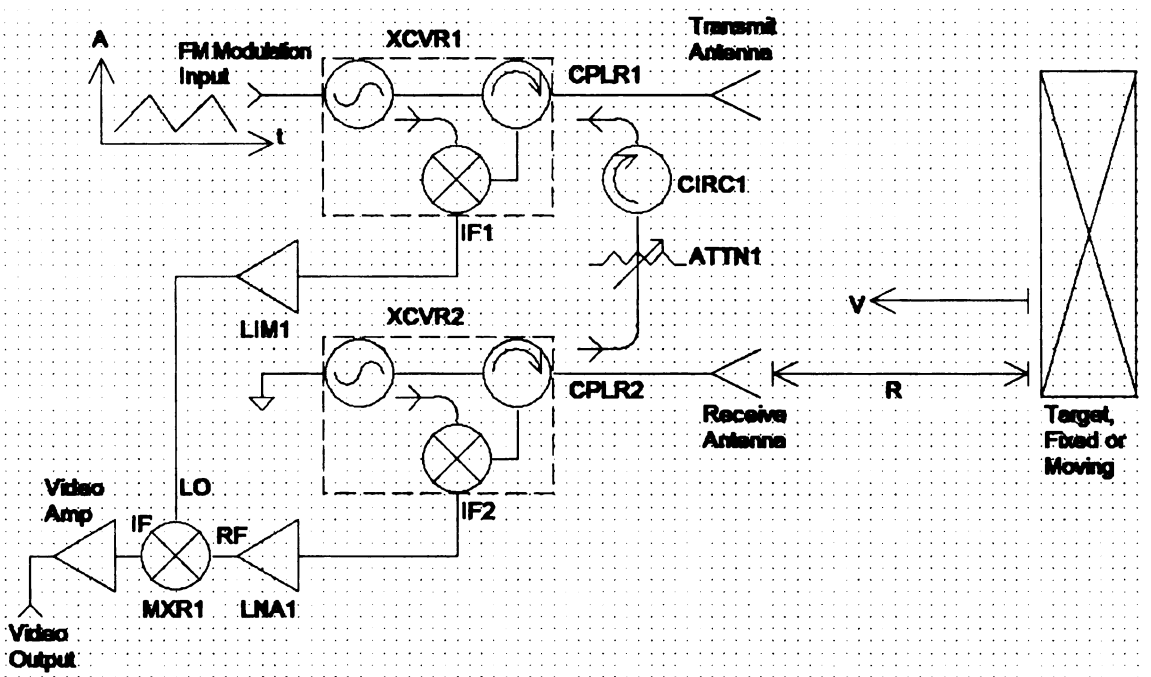

Figure 4.4: Simplified block diagram of the unique FMCW radar solution.

A simplified block diagram of the unique FMCW radar solution is shown in figure 4.4. XCVR1 is centered at frequency f_1 and FM modulated with a linear chirp $m(t)$, which causes a frequency deviation of $\phi(t)$. The frequency deviation $\phi(t)$ can be found using the following equations [15]:

$$\frac{d\phi}{dt} = k_f m(t) \tag{4.1}$$

Where: k_f = the frequency deviation constant, expressed in radians per second per unit of $m(t)$

$m(t)$ = the modulation waveform which is frequency modulating XCVR1 (in this case, it is a linear ramp)

The frequency deviation constant, k_f, can be found using the equation:

$$k_f = 2\pi f_d \tag{4.2}$$

Where: f_d = the frequency deviation constant of the modulator, and is expressed in hertz per unit of $m(t)$

The frequency deviation $\phi(t)$ can be expressed using the equation:

$$\phi(t) = k_f \int_{t_0}^{t} m(\alpha) d\alpha + \phi_0 \tag{4.3}$$

Where: t = time

t_0 = initial time

ϕ_0 = phase deviation at time $t = t_0$

Finally, the output of XCVR1 is represented with the equation:

$$TX_1(t) = A_c \cos[2\pi f_1 t + \phi(t)] \tag{4.4}$$

The output of XCVR1 is fed into the transmit antenna. The transmitted signal is reflected off of the target. The target is situated at a range R and moving at a velocity v (if it is moving). The range R and velocity v correspond to a time difference and Doppler shift between the original transmit signal and that which was picked up by the receive antenna and fed into XCVR2. This time difference corresponds to a beat frequency difference f_b as was proven in section 2.2. Thus, the reflected signal from the target is represented by the equation:

$$TX_{1b}(t) = A_c \cos[2\pi f_1 t + \phi(t) + 2\pi f_b t] \tag{4.5}$$

XCVR2 is set to a fixed frequency of f_2. XCVR2 is radiating a fixed frequency carrier at that frequency which can be represented by the equation:

$$TX_2(t) = A_c \cos[2\pi f_2 t] \tag{4.6}$$

As explained in section 4.1, the IF output of each transceiver module is a product of its VCO frequency and any RF power that is coming into the input/output port of the module. Because of this, the IF output of XCVR2 can be calculated:

$$IF_2(t) = TX_{1b}(t) TX_2(t)$$

$$= A_c^2 \cos[2\pi f_1 t + \phi(t) + 2\pi f_b t] \cos[2\pi f_2 t]$$

$$= \frac{A_c^2}{2}\cos[2\pi f_1 t + \phi(t) + 2\pi f_b t + 2\pi f_2 t] + \\ + \frac{A_c^2}{2}\cos[2\pi f_1 t + \phi(t) + 2\pi f_b t - 2\pi f_2 t] \tag{4.7}$$

The higher frequency term can be dropped. This is a practical consideration since the IF output port of the transceiver modules is not capable of producing X-band microwave signals. Thus, the IF output of XCVR2 can be simplified as:

$$IF_2(t) = \frac{A_c^2}{2}\cos[2\pi f_1 t + \phi(t) + 2\pi f_b t - 2\pi f_2 t] \tag{4.8}$$

Simultaneously, some power from XCVR2 is coupled into XCVR1. Power from XCVR2 is coupled out using CPLR2 and output through ATT1, CIRC1, and into CPLR1. The coupled power injected into CPLR1 is fed into XCVR1. The resulting frequency response at the IF port of XCVR1 is calculated using the equation:

$$IF_1(t) = TX_2(t)TX_1(t)$$

$$= A_c^2 \cos[2\pi f_2 t]\cos[2\pi f_1 t + \phi(t)]$$

$$= \frac{A_c^2}{2}\cos[2\pi f_2 t + 2\pi f_1 t + \phi(t)] + \\ + \frac{A_c^2}{2}\cos[2\pi f_2 t - 2\pi f_1 t - \phi(t)] \tag{4.9}$$

Like XCVR2, the higher frequency term can be dropped. Thus, the IF output of XCVR1 can be simplified as:

$$IF_1(t) = \frac{A_c^2}{2}\cos[2\pi f_2 t - 2\pi f_1 t - \phi(t)] \tag{4.10}$$

$IF_1(t)$ is fed into the input port of a limiting amplifier, LIM1. The output of LIM1 is used as the LO drive of MXR1. $IF_2(t)$ is fed into the input port of an LNA, which is represented by LNA1. The output of LNA1 is fed into the RF input port of MXR1. $IF_1(t)$ and $IF_2(t)$ are multiplied together in MXR1. The IF output of MXR1 is amplified by a video amplifier. The resulting product from MXR1 can be represented by the equation:

$$\text{Video Output} = IF_1(t)IF_2(t)$$

$$= \frac{A_c^4}{4}\cos[2\pi f_2 t - 2\pi f_1 t - \phi(t)]\cos[2\pi f_1 t + \phi(t) + 2\pi f_b t - 2\pi f_2 t]$$

$$= \frac{A_c^4}{4}\cos[2\pi f_2 t - 2\pi f_1 t - \phi(t) + 2\pi f_1 t + \phi(t) + 2\pi f_b t - 2\pi f_2 t] +$$

$$+ \frac{A_c^2}{4}\cos[2\pi f_1 t + \phi(t) + 2\pi f_b t - 2\pi f_2 t - \phi(t) + 2\pi f_b t - 2\pi f_2 t]$$

$$= \frac{A_c^4}{4}\cos[2\pi f_b t] + \frac{A_c^4}{4}\cos[-4\pi f_2 t - \phi(t) + 2\pi f_b t] \qquad (4.11)$$

The IF port of MXR1 is not capable of reproducing the high frequency term from equation 4.8. Therefore the video output of the radar system can be expressed as:

$$\text{Video Output} = \frac{A_c^4}{4}\cos[2\pi f_b t] \qquad (4.12)$$

It is clear from the equation above, that the video output is the beat frequency difference f_b due to distance from target R and velocity of target v. Thus, we have an FMCW radar system using two inexpensive microwave transceiver modules.

It should be noted that when the FM modulation $k = 0$, the system will function as a CW Doppler radar. Thus causing the video output equation to become:

$$\text{Video Output} = \frac{A_c^4}{4}\cos[2\pi f_d t] \tag{4.13}$$

Where f_b becomes f_d when there is no chirp, from equations 2.6 and 2.7.

A unique and low cost FMCW radar system has been proven. This system is theoretically capable of both FMCW and CW Doppler operation. Unwanted antenna coupling described in chapter 3 is used to the advantage of this radar system. The system deliberately forces antenna coupling for use as a reference LO for MXR1. One further advantage to this system is that the delay lines required to cancel any further unwanted coupling can be installed in series with IF1 and IF2, allowing for the use of low frequency and low cost delay lines.

4.3 System Design and Implementation

A unique FMCW radar solution was presented in section 4.2. The actual implementation of this system will be explored in this section. The system is composed of five major components. These components include the front end assembly, power supply, IF chassis, data acquisition and trigger, and the software. The entire system block diagram is shown in figure 4.5. A picture of the system can be seen in figure 4.6.

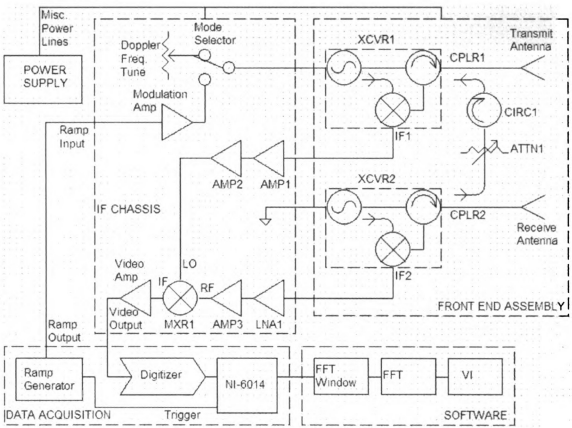

Figure 4.5: System block diagram.

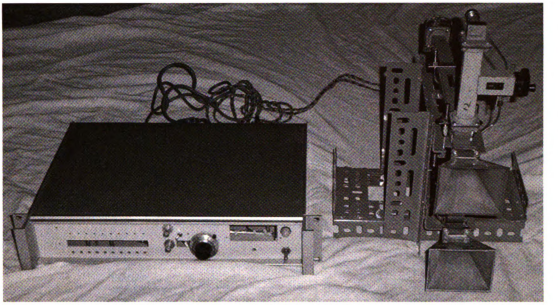

Figure 4.6: FMCW radar system.

4.3.1 The Front End Assembly

The unique solution to FMCW radar has a very unusual front end. The front end assembly creates the chirp, transmits it, and receives the reflected signal. The front end assembly is also where the forced coupling between XCVR1 and XCVR2 occurs. A block diagram of the front end assembly is shown in figure 4.7, and a picture of it is shown in figure 4.8.

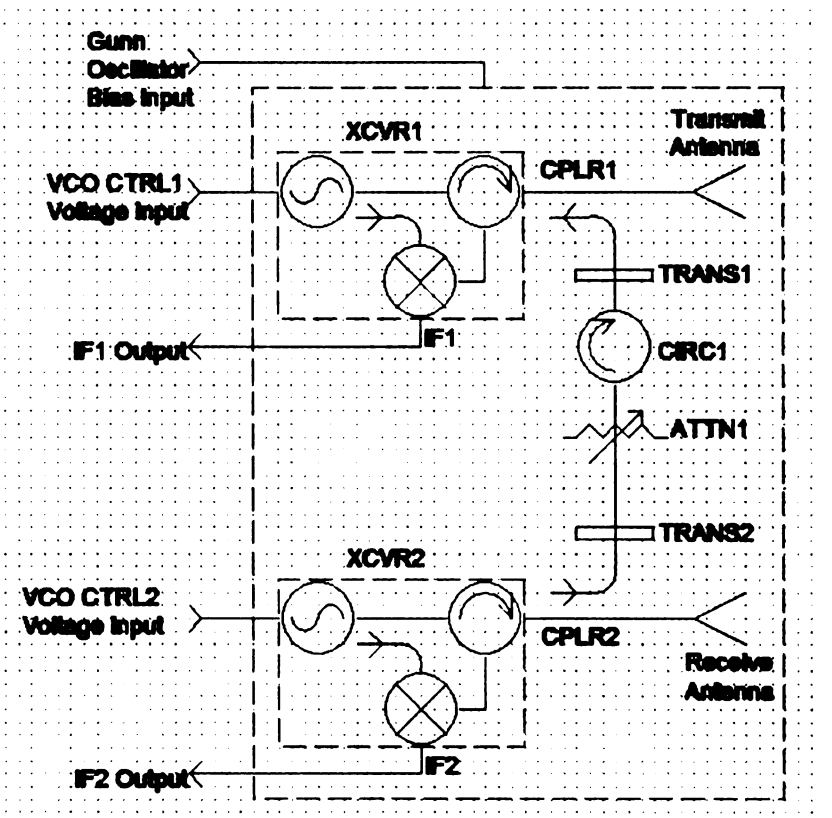

Figure 4.7: Front end assembly block diagram.

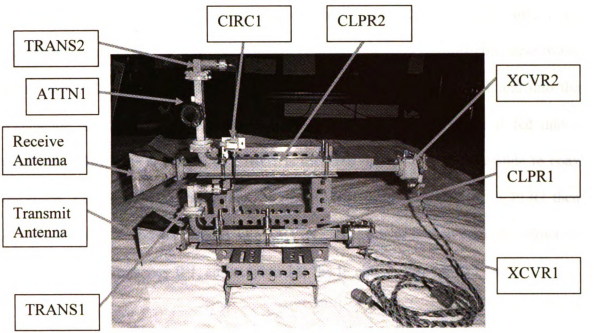

Figure 4.8: The front end assembly.

The Front end assembly creates a transmit chirp using an X-band microwave transceiver module, XCVR1. The transmit chirp is created when the varactor diode controlled Gunn oscillator of XCVR1 is modulated with a linear ramp which is fed in from the IF chassis to VCO CTRL1. The input/output port of XCVR1 is connected to the directional coupler CLPR1. CPLR1 is then fed into the transmit antenna. The chirp signal is transmitted out of the transmit antenna, bounced off of the target, and is reflected back into the receive antenna. The receive antenna is fed into the directional coupler CPLR2. CPLR2 is then fed into the input/output port of an X-band microwave transceiver module, XCVR2. XCVR2 is set to a fixed frequency through biasing VCO CTRL2, and converts the entire chirp bandwidth down to an intermediate frequency. That intermediate frequency is then outputted to the IF chassis through IF2.

The forc

frequenc

attenuato

waveguic

circulato

transitior

couples s

an interm

The Gun

from Gu

oscillator

XCVR1

microwa

were des

in figure

The forced coupling occurs between CPLR1 and CPLR2. XCVR2 is set to a fixed frequency. Some power from XCVR2 is coupled out to the adjustable microwave attenuator ATT1 through CPLR2. That power is then fed out of ATT1 and into the waveguide to coax transition TRANS2. The coaxial port of TRANS2 is fed into a circulator, CIRC1. The output of CIRC1 is then fed into a second waveguide to coax transition, TRANS1. The waveguide end of TRANS1 is fed into CPLR1. CPLR1 then couples some of the power directly into XCVR1. That power is then converted down to an intermediate frequency IF1, and outputted to the IF chassis through IF1 Out.

The Gunn oscillators of both XCVR1 and XCVR2 are powered with a DC bias voltage from Gunn Oscillator Bias Input. Both transceivers are biased such that their Gunn oscillators are in oscillation.

XCVR1 and XCVR2: Both XCVR1 and XCVR2 are M/A-Com MA87127-1 X-band microwave transceiver modules. The operational details of these transceiver modules were described in chapter 4.1. The connections made to XCVR1 and XCVR2 are shown in figure 4.9.

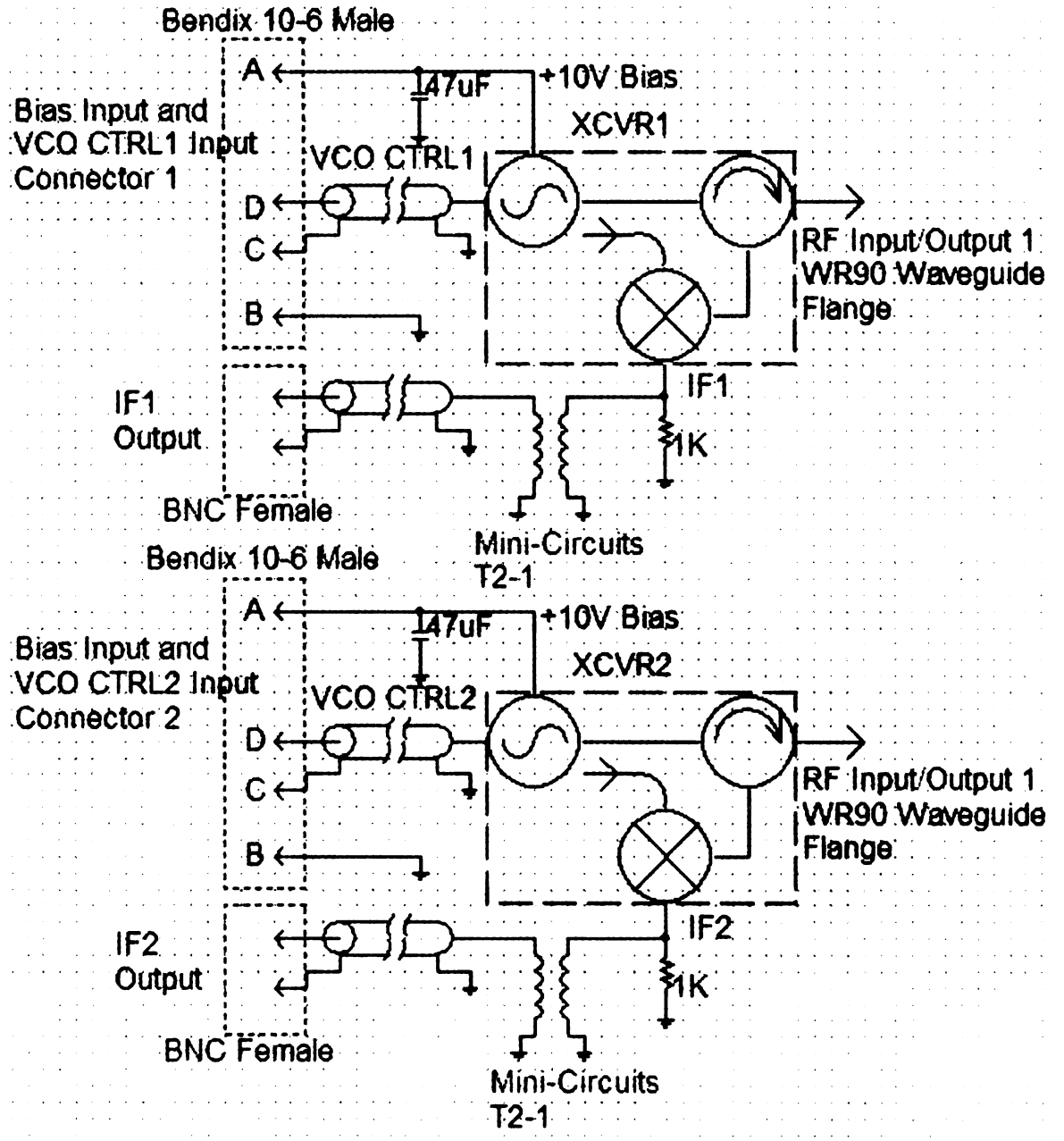

Figure 4.9: Schematic of XCVR1 and XCVR2 interconnections.

Looking at figure 4.9, XCVR1 is biased with +10 V from the power supply which is fed into the XCVR module through pin A of Bias and VCO CTRL1 Connector 1. This connector is a Bendix model 10-6 connector. The bias voltage is filtered with a 47uF cap, and then tied to the Gunn diode bias terminal on XCVR1. The bias ground is fed

from the power supply to XCVR1 through pin B of the 10-6 connector. The ground wire is then tied to the chassis of XCVR1. The VCO control voltage, VCO CTLR1, originates from the IF chassis. VCO CTRL1 is fed in through pins D and C of the 10-6 connector. Pin D connects to the center conductor of a RG174 coax cable. Pin C connects to the shield of that cable. At the end of the length of RG174, the center conductor is tied to the varactor diode terminal on XCVR1. The shield of the coax is tied to the chassis of XCVR1. The IF output of XCVR1, IF1, is fed out of the module through a solder pin. That pin is tied to a 1 K Ohm resistor, which is tied to ground. The 1 K Ohm resistor protects the IF output of XCVR1. The IF output pin is then connected to the primary winding of a 2:1 impedance matching transformer. The transformer is a Mini-Circuits model T2-1. The secondary winding is then connected to a BNC female connector. That BNC connector is the IF1 output port.

Much the same as XCVR1, XCVR2 is biased with +10 V from the power supply which is fed into the XCVR module through pin A of Bias and VCO CTRL2 Connector 2. This connector is a Bendix model 10-6 connector. The bias voltage is filtered with a 47uF cap, and then tied to the Gunn diode bias terminal on XCVR2. The bias ground is fed from the power supply to XCVR2 through pin B of the 10-6 connector. The ground wire is then tied to the chassis of XCVR2. The VCO control voltage, VCO CTLR2, originates from the IF chassis. VCO CTRL2 is fed in through pins D and C of the 10-6 connector. Pin D connects to the center conductor of a RG174 coax cable. Pin C connects to the shield of that cable. At the end of the length of RG174, the center conductor is tied to the varactor diode terminal on XCVR2. The shield of the coax is tied to the chassis of

XCVR2. The IF output of XCVR2, IF2, is fed out of the module through a solder pin. That pin is tied to a 1 K Ohm resistor, which is tied to ground. The 1 K Ohm resistor protects the IF output of XCVR2. The IF output pin is then connected to the primary winding of a 2:1 impedance matching transformer. The transformer is a Mini-Circuits model T2-1. The secondary winding is then connected to a BNC female connector. That BNC connector is the IF2 output port.

CLPR1 and CLPR2: CLPR1 and CLPR2 are both X-band directional couplers of unknown part numbers and an unknown origin (see figure 4.8). They were purchased as government surplus. When tested, both couplers had a coupling factor of -10 dB. Both couplers use WR90 waveguide flange connections for all ports.

TRANS1 and TRANS2: TRANS1 and TRANS2 are both WR90 to type N female connector transitions (see figure 4.8). These transitions were tested, and found to be functional over the entire operational bandwidth of the radar system. The transitions are government surplus, and the part numbers and origin of these transitions is unknown.

Transmit Antenna and Receive Antenna: The transmit and receive antennas are both M/A-Com model number MA86551 (see figure 4.10). Both are horn antennas with a WR90 waveguide feed. The operational frequency range of these antennas is 8 GHz to 12.4 GHz. The H-plane and E-plane 3 dB beamwidths are specified to be 25 degrees. The nominal gain of these antennas is 17 dB.

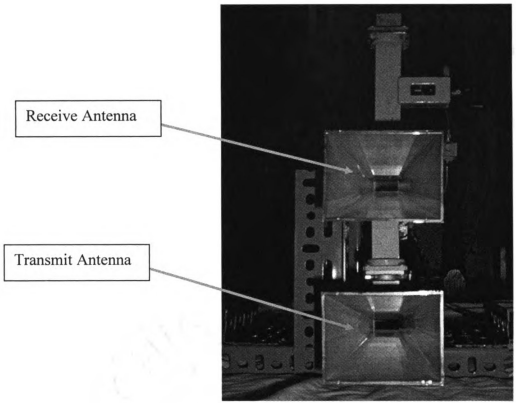

Figure 4.10: Transmit and Receive Antennas.

ATTN1: ATTN1 is a waveguide attenuator. Both the input and output ports of this attenuator are WR90 waveguide flange. The attenuator is adjusted with a manual knob, which can be seen in figure 4.8. The part number and origin of this attenuator is unknown since it is a government surplus component.

CIRC1: CIRC1 is a ferrite circulator set up as an isolator. CIRC1 is a coaxial part, where both the input and output ports are SMA female connectors (see figure 4.8). The isolation of CIRC1 was measured to be 10 dB. The part number and origin of this circulator is unknown.

4.3.2 The Power Supply

The power supply is a crucial part of the system. The power supply provides a number of voltages to power the various components of the system. These voltages include +10 V for the transceiver modules, +12 V for the RF amplifiers, +24 V for the modulation amplifier, and +/- 5V for the video amplifier. The power supply is located in the IF chassis (see figure 4.11). Figure 4.12 shows the power supply schematic.

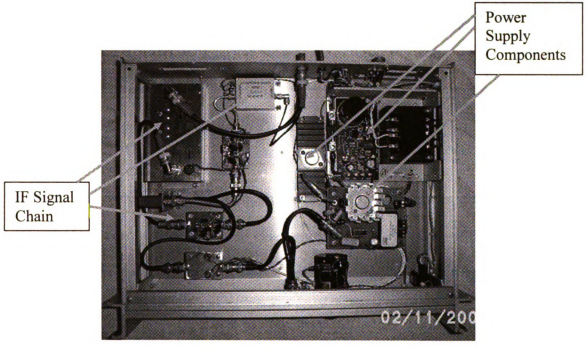

Figure 4.11: IF Chassis.

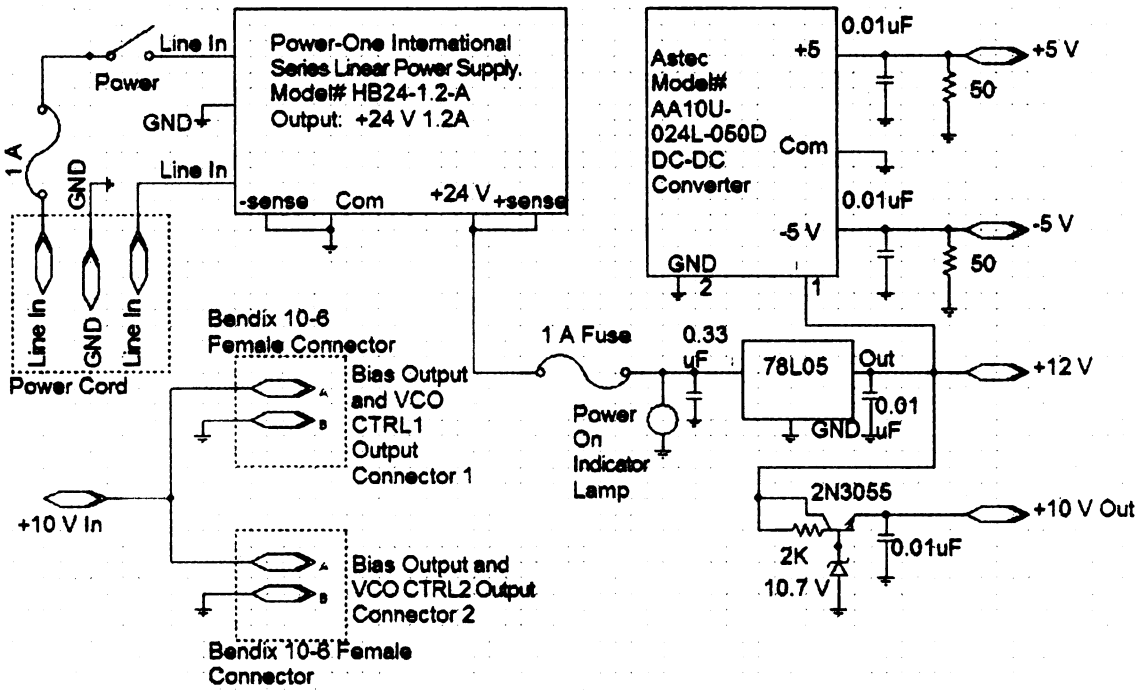

Figure 4.12: Power supply schematic.

120 VAC line voltage is fed in through a standard 3 prong power cord. The ground terminal of the cord is tied directly to chassis ground. The hot wire of the power cord is tired directly to a fuse as soon as it enters the IF chassis. The fuse is then tied to a main power switch. The other terminal of the power switch is tied to one of the line in terminals of the 24 VDC linear power supply. The other line in terminal on the power supply is tied directly to the neutral wire of the power cord. The linear power supply output is 24 VDC at 1.2 A. The output common terminal of the power supply is tied directly to ground. The +24 VDC output of the power supply is tied directly to a 1 A fuse. The other end of the fuse is fed to a power on indicator lamp, and then distributed throughout the system to anything requiring 24 VDC. A 12 V linear regulator is tied to the 24 VDC rail of the power supply. The regulator provides 12 V to anything that

requires it. A single transistor 10 V regulator is connected to the 12 V regulator output. The 10 V regulator provides bias voltage for XCVR1 and XCVR2. A DC to DC converter is also connected to the 12 V rail. The DC to DC converter creates +5 V and -5 V for the video amplifier. Careful attention is paid to laying out the line voltage wires in close proximity to the DC lines. The physical layout of the power supply is shown in figure 4.13.

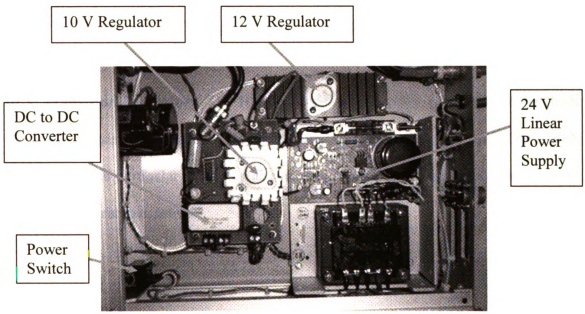

Figure 14.13: Physical layout of the power supply.

Linear Power Supply: The linear power supply is a Power-One model number HB24-1.2-A international series. This power supply is capable of supplying 24 VDC at 1.2 A of current. It also has remote sensing capabilities, which are simply bypassed in this application by tying –sense to the com, and +sense directly to the +24 V output terminal.

12 V Regulator: The 12 V regulator is a general purpose linear chip, the 78L12. This particular 78L12 uses a large TO-204 case for heat dissipation.

DC to DC Converter: The DC to DC converter is an Astec model number AA10U-024-050. This DC to DC converter is capable of dropping up to 36 VDC down to +5 VDC and -5 VDC. It is used exclusively to power the video amplifier. In this particular application, the video amplifier does not draw enough current to turn on the DC to DC converter, so load resistors were tied directly between the outputs and ground to provide enough current drain to turn on the converter in a stable operational mode.

10 V Transistor Regulator: The 10 VDC transistor regulator is a simple zener diode and NPN transistor regulator. This particular regulator uses a large 2N3055 NPN transistor. This particular transistor also uses a TO-204 case, similar to the 12 VDC regulator, for heat dissipation.

4.3.3 IF Chassis

The IF chassis is a critical part of the system. The IF chassis serves two purposes. It multiplies the IF from XCVR1 and XCVR2, producing a video output that consists only of target beat frequencies and Doppler shifts. It also amplifies and offsets the ramp modulation input to appropriate levels for the varactor diode VCO in XCVR1. An inside view of the IF chassis is shown in figure 4.11. The block diagram of the IF chassis is shown in figure 4.14.

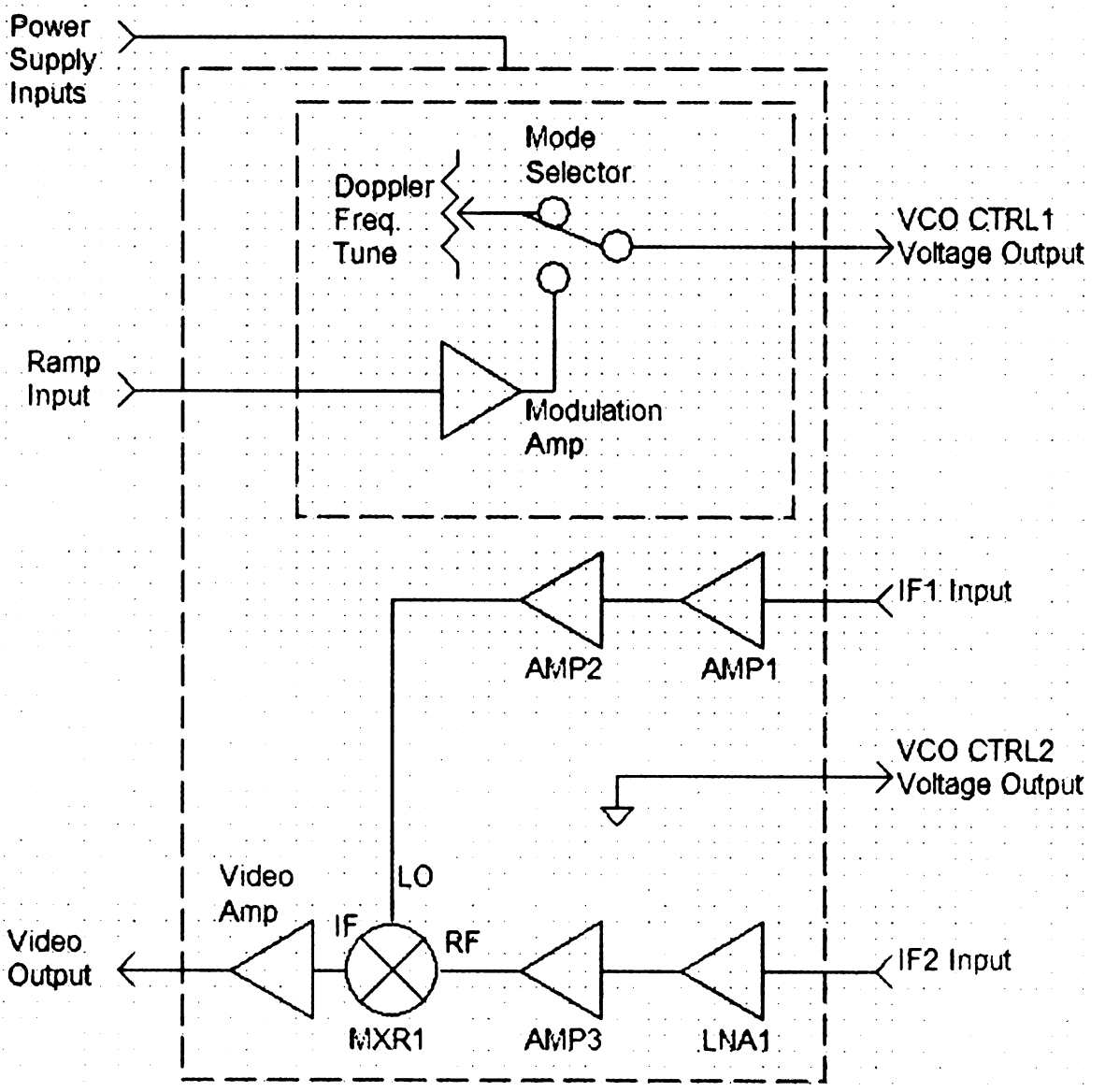

Figure 4.14: Block diagram of IF chassis.

The IF chassis physical layout is shown in figure 4.15.

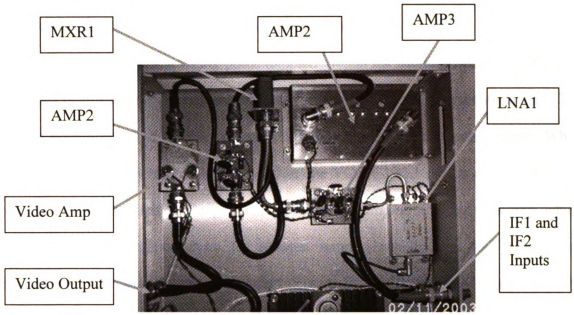

Figure 4.15: IF chassis physical layout.

When multiplying the IF from XCVR1 and XCVR2, the IF chassis takes in IF1 from XCVR1 and amplifies it to a mixer LO drive level of +7 dBm, and fed into the double balanced mixer, MXR1. This is achieved using two general purpose RF amplifiers, AMP1 and AMP2. IF2 takes a slightly different rout when it is fed into the IF chassis. IF2 is fed directly into a low noise amplifier, LNA1. The output of LNA1 is then fed into a general purpose RF amplifier, AMP3. The output of AMP3 is fed into the RF port of MXR1. When the LO and RF are mixed in MXR1, the resulting IF is then amplified with a video op amp, the Video Amp. The output of the Video Amp is fed out of the IF chassis through the Video Out connection. The Video Out is the range to target and Doppler shift information in the form of beat frequencies.

Two operational modes can be chosen using the Mode Selector. The Mode Selector is a two way switch. It can connect the VCO CTRL1 output port on the IF chassis to either the Modulation Amp or a tuning potentiometer. When the Mode Selector is in the CW Doppler position, the VCO CTRL1 port is connected to a tuning potentiometer. The tuning potentiometer is capable of tuning XCVR1 across its entire tuning range. When the Mode Selector is in the FMCW position, the VCO CTRL1 port is connected to the output of the Modulation Amp. The Modulation Amp is a simple op-amp which amplifies the modulation from an external ramp generator, and DC offsets that modulation waveform. The DC offset feature is adjustable, and allows the FM modulation to be centered around any desired frequency within the tuning range of XCVR1. The output port VCO CTRL2 on the IF chassis is tied to ground, since XCVR2 is left un-modulated.

AMP1: AMP1 is a general purpose surplus RF amplifier. It has a gain of approximately 20 dB between the frequency ranges of 10 MHz and 200 MHz. It requires a +12 VDC connection to the power supply. The RF input and output connections are both BNC female connectors. Other specifications on this amplifier are unknown since it is a surplus item of an unknown origin.

AMP2: AMP2 is a pair of Mini-Circuits MAV-2 MMIC amplifiers in series on a strip of 50 Ohm microstrip. The gain of these two amplifiers in series is approximately 25 dB from 100 KHz to above 1 GHz. The maximum IP1 output of this amplifier is +13 dBm at -12 dBm input. However, the IP1 is adjustable. The IP1 is adjusted using the

potentiometer connected to the LM317 voltage regulator. The LM317 allows for adjustment of the bias on the second MAV-2 amplifier. By lowering the bias on the MAV-2, the IP1 can be lowered. A low IP1 causes AMP3 to work as a limiting amplifier. This limiting amplifier drives the LO of MXR1. The RF input and output connections are both BNC female connectors. The schematic of this amplifier is shown in figure 4.16.

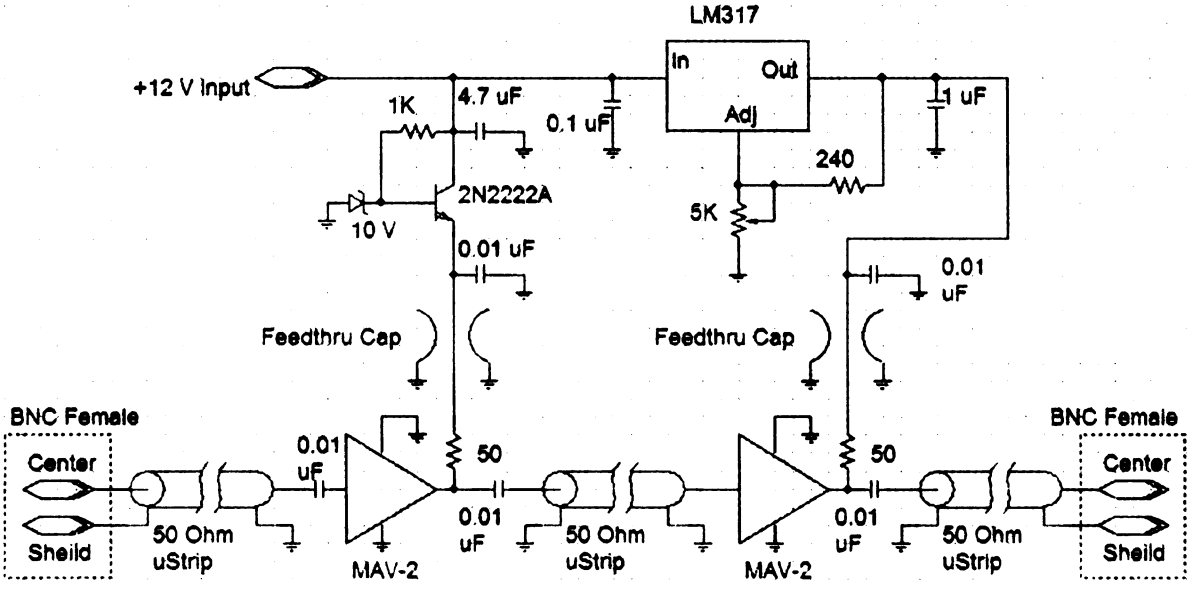

Figure 4.16: AMP2 schematic.

MXR1: MXR1 is a double balanced coaxial mixer. This mixer has an HP part number of HP10514A. This mixer requires an LO drive level of +7 dBm. It has an insertion loss of approximately 6 dB, and an input IP1 of +1 dBm. All of the ports, RF, LO, and IF are BNC female connectors.

LNA1: LNA 1 is a surplus RF low noise amplifier of an unknown origin. It has a gain of 25 dB across a frequency range of roughly 10 MHz to 250 MHz. Its IP1 output power is +10 dBm with -15 dBm of input power. Both the input and output ports are SMA female connectors.

AMP3: AMP3 is nearly identical to AMP2. AMP3 is a pair of Mini-Circuits MAV-2 MMIC amplifiers in series on a strip of 50 Ohm microstrip. The gain of these two amplifiers in series is approximately 25 dB from 100 KHz to above 1 GHz. The IP1 output of this amplifier is +13 dBm at -12 dBm input. The RF input connection is an SMA female connector. The RF output connection is a BNC female connector. The schematic of this amplifier is shown in figure 4.17.

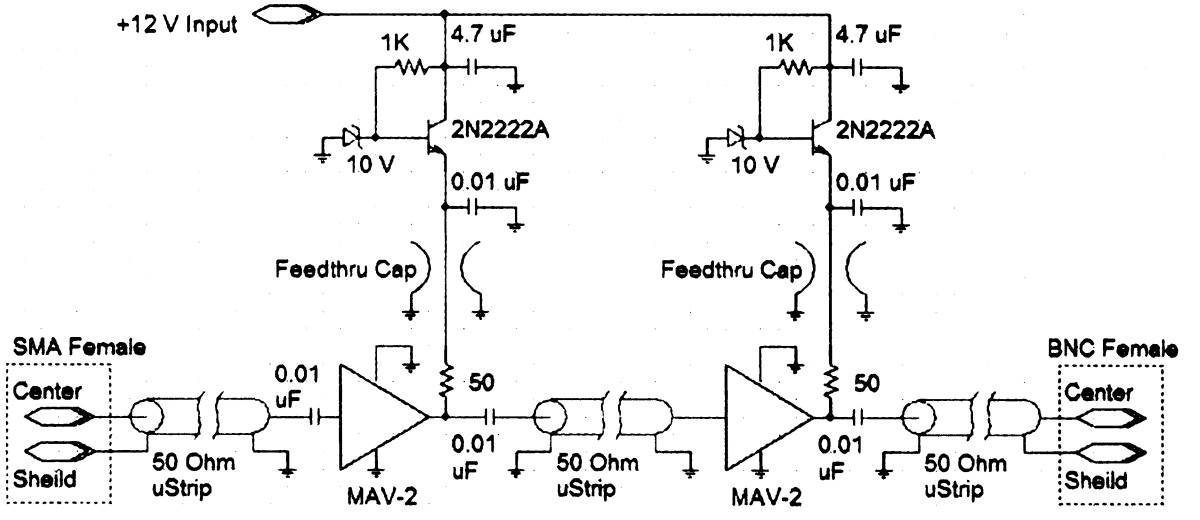

Figure 4.17: AMP3 schematic.

Video Amp: The Video Amp is the obsolete Maxim semiconductor MAX404. This video op-amp has a maximum bandwidth of 80 MHz, and is built in an 8 pin DIP package. In the Video Amp circuit, the MAX404 is set up for an AC gain of 8. The circuit is setup to take a source impedance of 50 Ohms, which is terminated by a 50 Ohm resistor on the MAX404 input terminals. The output impedance of this circuit is 50 Ohms set by a resistor in series with the output terminal of the MAX404. A schematic of the Video Amp is shown in figure 4.18.

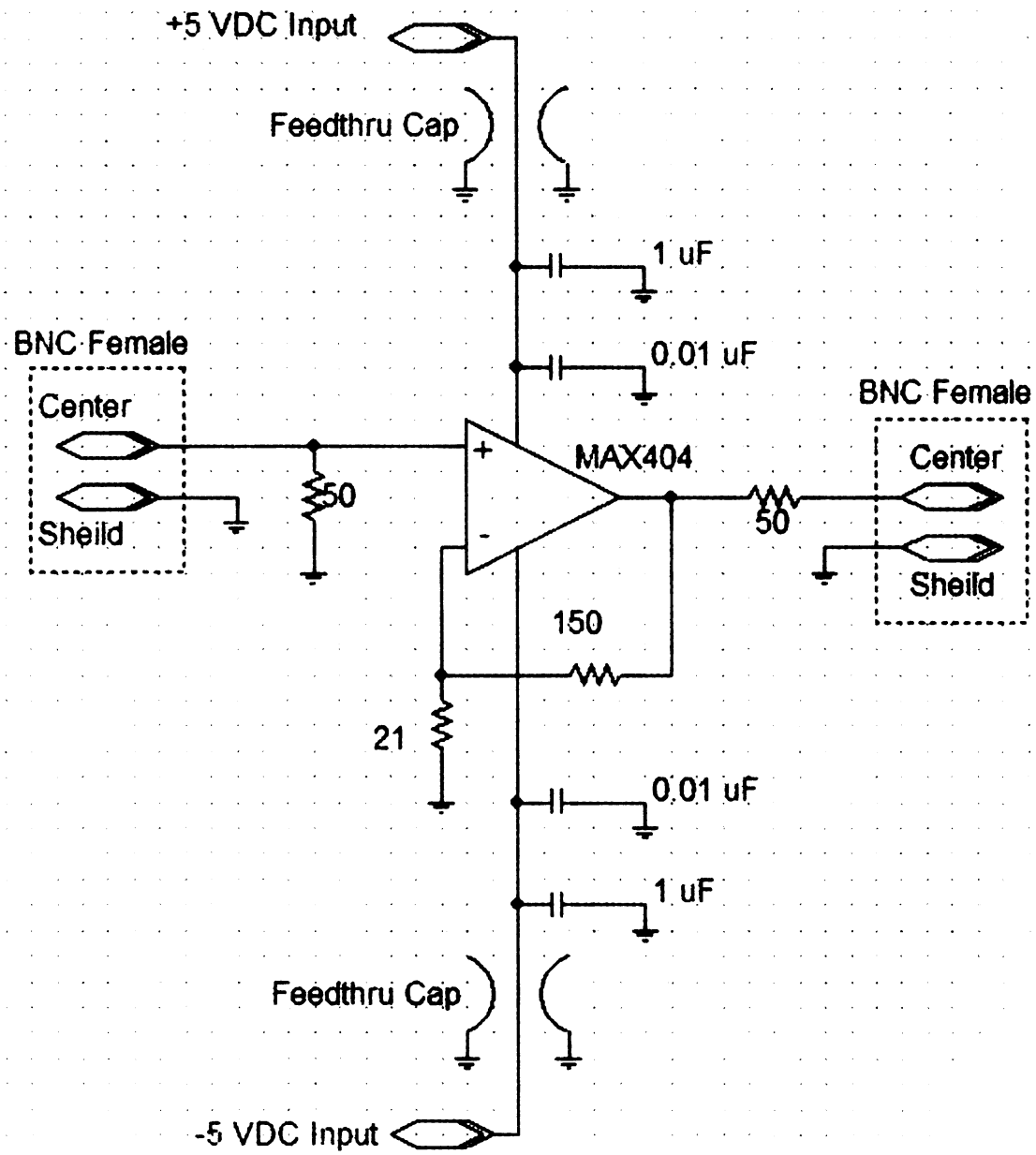

Figure 4.18: Video Amplifier Schematic.

Modulation Amp: The Modulation Amp shares a circuit board with the 10 V regulator and the DC to DC converter components of the power supply (see figure 4.13). The Modulation Amp is based around an LM324 single supply quad op-amp. Only one op-amp out of the 4 available on the chip is used. The LM324 was chosen because of its

reliable single ended performance, and ability to swing over 20 V from its output. The schematic of the Offset Amplifier and the Modulation amplifier is shown in figure 4.19. The LM324 is powered with a single supply of 24 VDC. The modulation input is brought in through the Ramp Input port on the IF chassis. The Ramp Input port is terminated with a 2.2 K Ohm resistor. The Ramp Input is then AC coupled through a 1 uF capacitor into the LM324 op-amp. The relatively high 1 uF capacitor was chosen because the design requires the use of a low frequency modulation input. At the input of the op-amp, a DC offset is introduced. This DC offset is adjustable with a 10 K Ohm trimmer pot. The op-amp is setup for a voltage gain of approximately 11. The output of the op-amp is fed into the FMCW mode side of the Mode Selector switch. The Mode Selector switch is a 2 way switch, capable of transferring the VCO CTRL1 Output port between the op-amp and a DC tuning potentiometer. The DC tuning potentiometer is setup as a voltage divider, where the input is regulated to a voltage output of 20 VDC. It is capable of outputting anywhere between 0 VDC and 20 VDC. The output of this circuit is fed into the CW Doppler mode position of the Mode Selector switch.

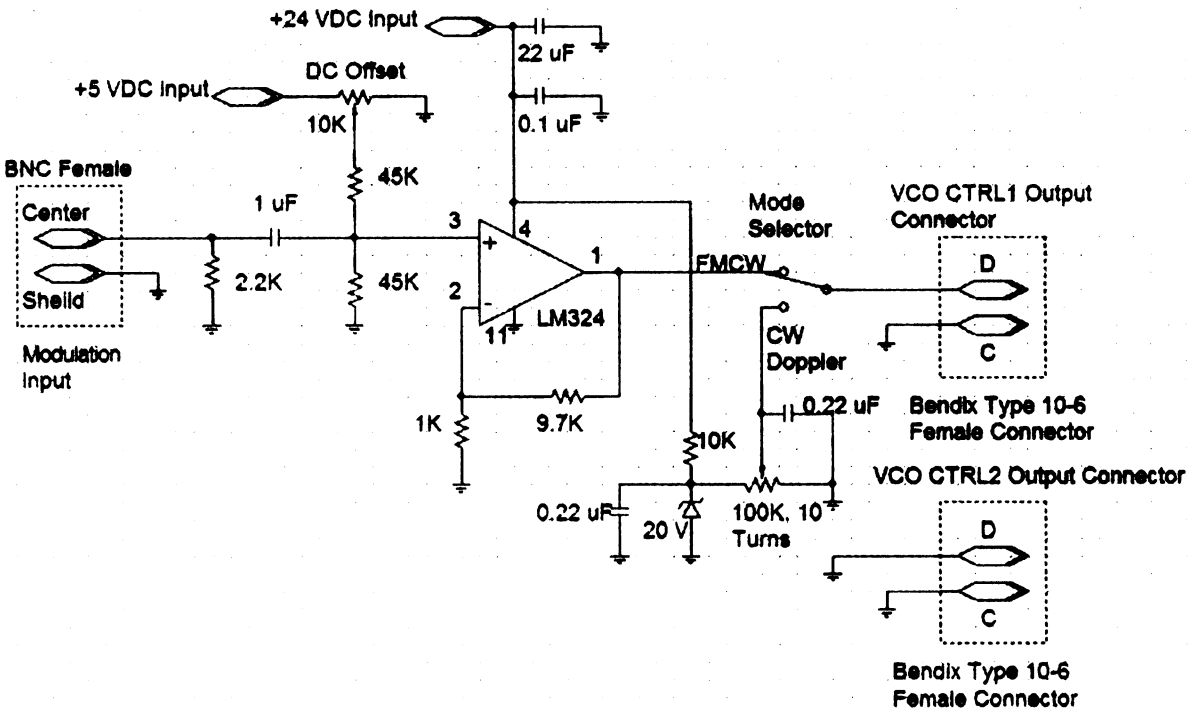

Figure 4.19: Modulation amplifier schematic.

4.3.4 Data Acquisition

The data acquisition system acquires the Video Output from the IF Chassis, and triggers the Ramp Generator (see figure 4.20). Data acquisition is achieved by use of a National Instruments NI6014 PCI card installed in a PC. Analog input channel 0 from the NI6014 is connected directly to the Video Output from the IF Chassis (see figure 4.21). Digital IO channel 0 from the NI6014 is connected directly to the trigger input of an HP3312A function generator set to produce a 100 Hz linear ramp. The analog input being used on the NI6014 is capable of 200 K samples per second, at a resolution of 16 bits.

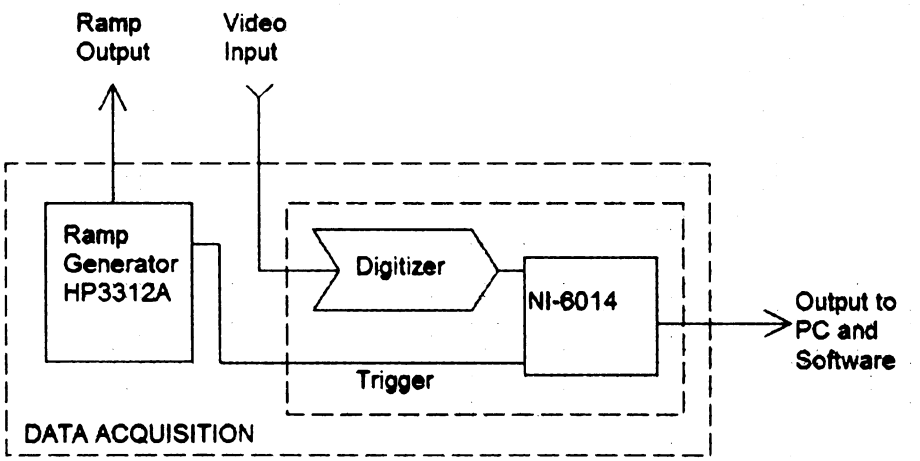

Figure 4.20: Block diagram of the Data Acquisition signal chain

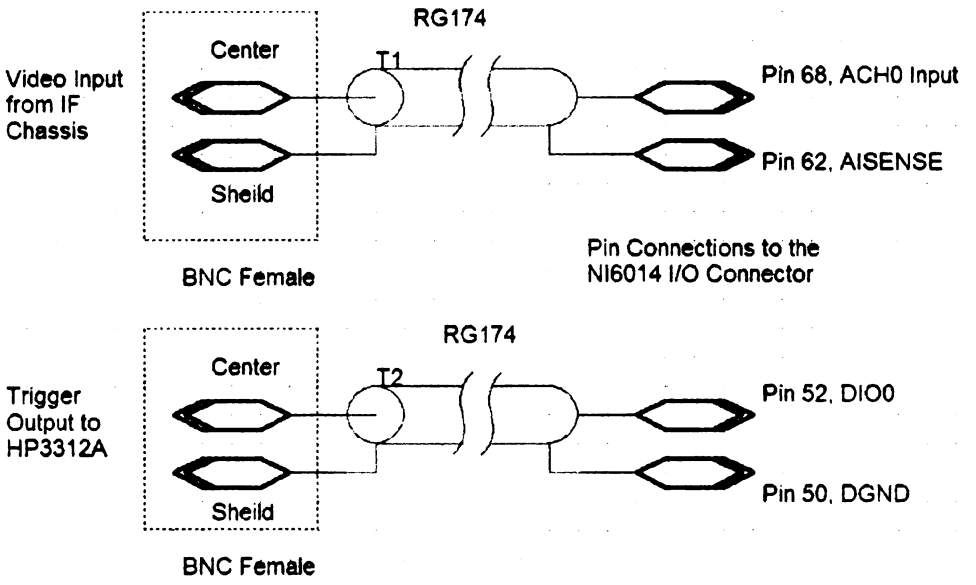

Figure 4.21: Schematic of NI6014 input and output connections.

4.3.5 Software

The software written for this radar system was coded using National Instruments LabVIEW Student Edition. LabVIEW is a symbolic programming language created by National Instruments. LabVIEW code looks much like a schematic, where various pieces of code are wired together to form a program. LabVIEW interfaces directly with National Instruments data acquisition products so that complex data acquisition and signal processing programs can be created using the symbolic programming environment of LabVIEW. A LabVIEW program that interfaces with instruments outside of the computer is known as a Virtual Instrument (VI). In the case of this radar system, all VI's were written to interface with the National Instruments NI6014 data acquisition PCI card.

Three VI's were created to run the radar system. A VI was created to continuously operate and display range information. A second VI was created to perform a single range profile capture. A third VI was created to operate the radar system as a Synthetic Aperture Radar.

Continuous Operation and Display: The Continuous Operation and Display VI was created in order to continuously operate the radar system and display range data in near real time. This program is used to monitor and adjust the radar system characteristics. It is also used for aligning standard radar targets. The VI causes the NI6014 to trigger the ramp generator and sample the Video Output from the IF Chassis. This sequence of operations is done repeatedly until the program is stopped.

The VI front panel (see figure 4.22) consists of a sample rate digital control, number of samples digital control, a scaled sample window control, two waveform graphs, and a stop button. The sample rate digital control sets the sample rate of the digitizer (up to 200 KSPS) on the NI6014. The number of samples digital control sets the number of samples collected by the NI6014. The scaled sample window control selects between 7 different scaled sample window types, including Hanning, Hamming, Blackman-Harris, Exact Blackman, Blackman, Flat Top, Four Term Blackman-Harris, and Seven Term Blackman Harris. Waveform graph 1 displays the time domain waveform that is fed into a Fast Fourier Transform (FFT) sub VI. Waveform graph 2 displays the magnitude of the FFT of the Video Output data. The stop button stops the program.

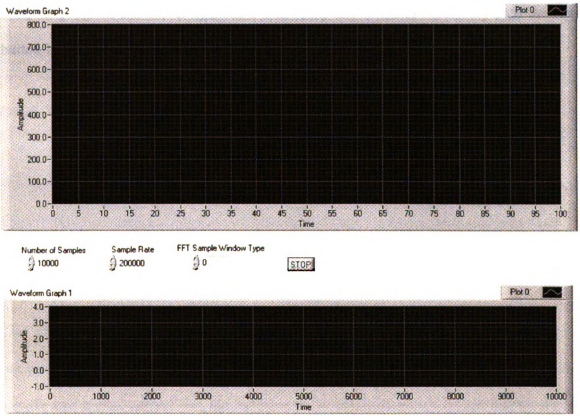

Figure 4.22: Continuous Operation and Display VI front panel.

The VI block diagram is shown in figure 4.23. When the VI is run, the program first turns off the ramp generator trigger line. It then waits 250 ms and turns on the ramp generator trigger line. On the rising edge of the ramp trigger line, the ramp generator starts a linear ramp which modulates the radar system. When the ramp generator is triggered, the data acquisition case statement is set to true and instructs the digitizer on the NI6014 to collect a specified number of samples at a specified rate which is selected by the user. After data is acquired, the data is then put through a selectable scale window. After the scale window, the data is padded with 9000 0's. This padded data is plotted on waveform graph 1 then fed into an FFT sub VI. The absolute value of the real output of the FFT sub VI is then plotted on waveform graph 2. After plotting the FFT data, the program starts over again in a while loop and executes repeatedly until the stop button is pressed on the front panel of the VI.

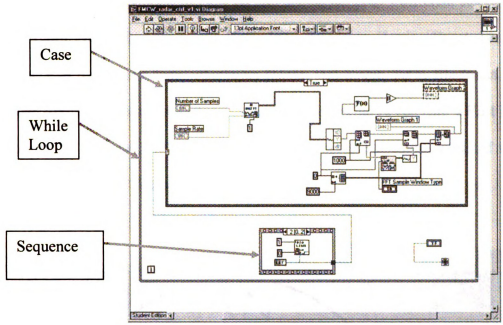

Figure 4.23: Continuous Operation and Display VI block diagram.

Single Range Profile Capture: The Single Range Profile Capture VI was created in order to capture and save a single magnitude range profile from the radar system. A range profile is defined as the raw range to target(s) information from a radar system. The VI triggers one ramp from the ramp generator to modulate the radar system and at the same time it digitizes the Video Output from the IF chassis. This data is then displayed and stored in a spreadsheet file. The VI only runs one time and then must be reset.

The VI front panel (see figure 4.24) consists of a sample rate digital control, number of samples digital control, a scaled sample window control, and two waveform graphs. The sample rate digital control sets the sample rate of the digitizer (up to 200 KSPS) on the NI6014. The number of samples digital control sets the number of samples collected by

the NI6014. The scaled sample window control selects between 7 different scaled sample window types, including Hanning, Hamming, Blackman-Harris, Exact Blackman, Blackman, Flat Top, Four Term Blackman-Harris, and Seven Term Blackman Harris. Waveform graph 1 displays the time domain waveform that is fed into a Fast Fourier Transform (FFT) sub VI. Waveform graph 2 displays the absolute value of the real output of the FFT of the Video Output data.

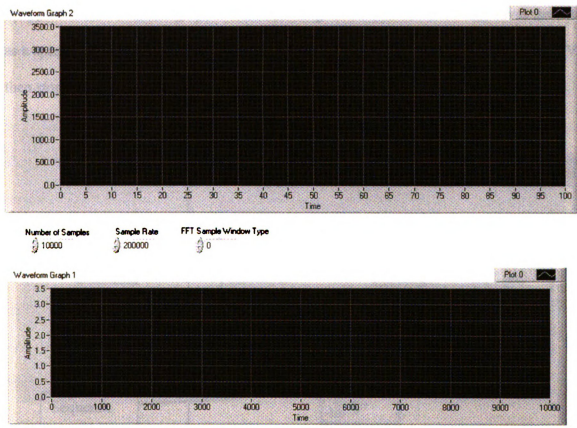

Figure 4.24: Single Range Profile Capture VI front panel.

The VI block diagram is shown in figure 4.25. This VI is very similar to the Continuous Operation and Display VI. When the VI is run, the program first turns off the ramp generator trigger line. It then waits 250 ms and turns on the ramp generator trigger line.

On the rising edge of the ramp trigger line, the ramp generator starts a linear ramp which modulates the radar system. When the ramp generator is triggered, the data acquisition case statement is set to true and instructs the digitizer on the NI6014 to collect a specified number of samples at a specified rate which is selected by the user. After data is acquired, the data is then put through a selectable scale window. After the scale window, the data is padded with 9000 0's. This padded data is plotted on waveform graph 1 then fed into an FFT sub VI. The magnitude of the complex output from the FFT sub VI is then plotted on waveform graph 2. After plotting the FFT data, the VI then saves the data as a spreadsheet file and prompts the user for a file name and location to store it. The VI then stops execution.

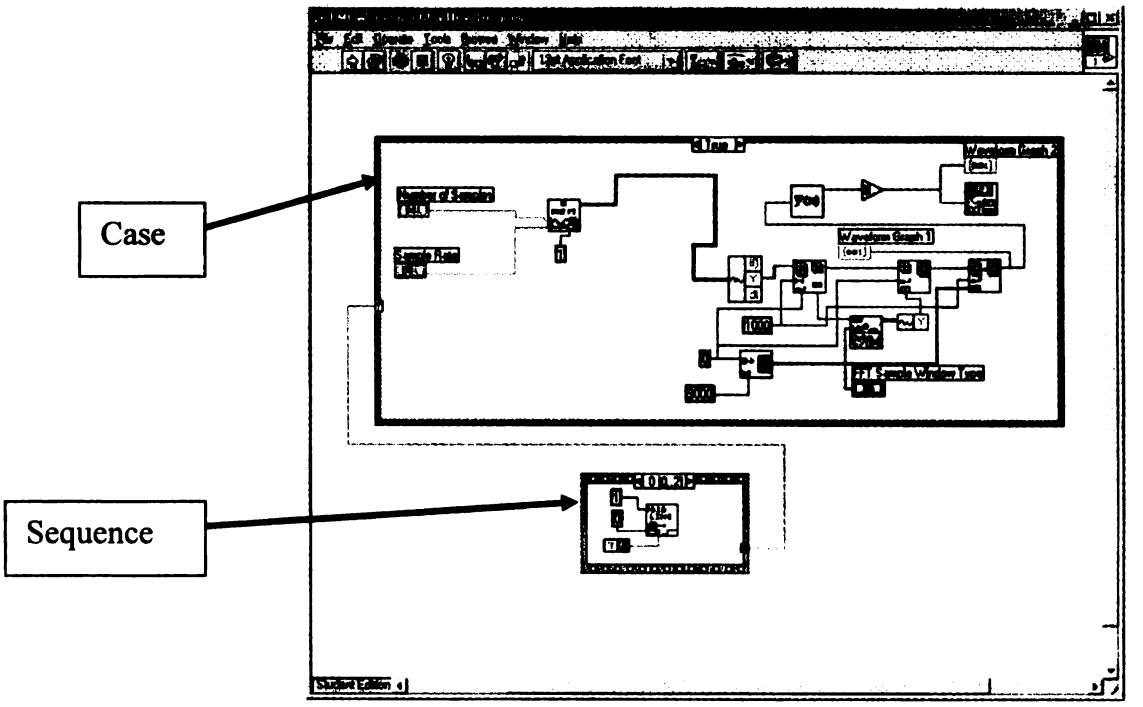

Figure 4.25: Single Range Profile Capture VI block diagram.

Synthetic Aperture Radar: The Synthetic Aperture Radar VI was written in order to create detailed SAR radar images using the unique FMCW radar solution. Creating a detailed SAR image would prove the viability of the unique radar solution for use in many advanced applications.

The SAR VI works with the hardware and the user to create a SAR image. The SAR VI controls the radar system by triggering the ramp generator, and by digitizing the Video Output from the IF chassis. The VI prompts the user to manually move the radar system down a metal track (see figure 4.26).

Figure 4.26: The SAR VI depends on the user to manually move the radar down a metal track.

The program acquires data at one location on the track at a time. The user specifies how many "beams" are to be collected. Beams refers to range profiles, the term "beams" was

used during the programming of the VI. The user then specifies the spacing between each beam, and the number of beams per synthetic aperture. The VI prompts the user to move the radar down the track one increment, and then collects data when the user hits the 'Enter' key. The radar is then chirped, and data is collected. The user is prompted to do the same again. This process is repeated until the specified number of beams (range profiles) are collected.

The VI front panel consists of many controls and output indicators (see figure 4.27). There are a total of 3 waveform graphs, 6 digital controls, and 3 digital indicators. The waveform graph at the top of the VI front panel plots all of the real components from each beam of data provided by the data acquisition loop. The waveform graph just below that one plots all of the imaginary components from each beam of data provided by the data acquisition loop. The waveform graph at the very bottom of the VI front panel is used to plot the magnitude of the output of every single focused range profile calculated by the SAR process. These waveform graphs are used simply to indicate weather or not the data acquisition loop has successfully acquired all of the needed range profiles used to make the SAR process function properly, and to check weather or not the SAR process has successfully occurred. The sample rate digital control sets the sample rate of the digitizer (up to 200 KSPS) on the NI6014. The number of samples digital control sets the number of samples collected by the NI6014. The scaled sample window control selects between 7 different scaled sample window types, including Hanning, Hamming, Blackman-Harris, Exact Blackman, Blackman, Flat Top, Four Term Blackman-Harris, and Seven Term Blackman Harris. The total number of beams digital control sets the

total number of range profiles that will be collected by the VI. The spacing digital control sets the spacing between each range profile. The number of beams per aperture sets the number of elements in the N element synthetic arrays that will be created by the SAR process. The current beam count digital indicator shows the user what range profile number has just been acquired. The length of array digital indicator shows the user the length dimension of the SAR process output array. The width of array digital indicator shows the user the width dimension of the SAR process output array.

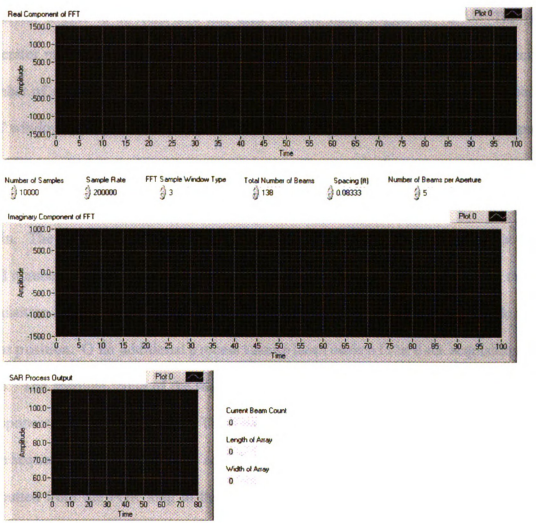

Figure 4.27: The Synthetic Aperture Radar VI front panel.

The SAR VI runs only once. It first acquires the specified number of range profiles. It then performs a SAR process on the acquired data. It then saves the data before and after SAR process.

The data acquisition loop acquires the specified number of 'beams' inputted by the user (see figure 4.28a). The term 'beams' refers to range profiles, but happened to be used in the programming of the SAR VI. When the program begins execution, it sets the ramp generator trigger to 0, waits 250 ms, then sets the ramp trigger to +5 V. The ramp generator modulates the radar. At this point in time, the program acquires the specified number of samples at the specified sample rate. The data is windowed by the specified FFT window type, padded with 9000 0's, then run through an FFT sub VI. The output of the FFT is split into real and imaginary arrays. The user is then prompted to move the radar and hit the 'enter' key to continue. When the enter key is hit, the process starts over again. The end result is a number of real and imaginary 1D arrays equal to that of the total number of beams inputted by the user. These 1D arrays are outputted from the data acquisition FOR loop to create two 2D arrays (real and imaginary) of range profile versus radar position. One additional process takes place inside of the data acquisition FOR loop. The absolute value of the real data is taken, so that the voltages of the frequency components can be determined. This result is outputted from the FOR loop to the file save sequence. This result is also scaled to the logarithmic radar range equation 2.5, and outputted from the FOR loop to the file save sequence. This data is saved in order to

show the data before the SAR process, so that it can be compared to data after the SAR process.

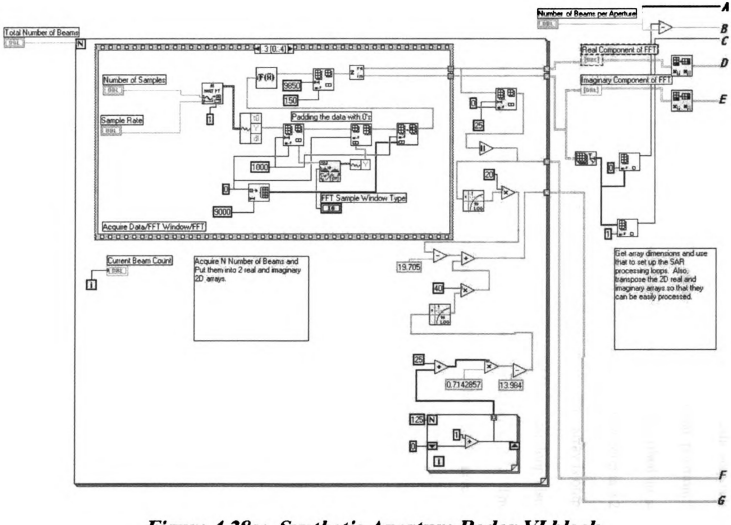

Figure 4.28a: Synthetic Aperture Radar VI block diagram, showing the data acquisition loop.

The Synthetic Aperture Radar process loop uses the data provided by the data acquisition loop to create a SAR image. The range profile data from the data acquisition loop is provided as two 2D arrays, real and imaginary data versus radar position. The SAR process loop (see figure 2.28b) executes the exact procedure described in section 2.3, using equations 2.15 through 2.20. The result from the SAR process loop is a 2D array of synthetic focused aperture magnitudes versus radar position. This array is outputted from the SAR process loop to the file save sequence. The SAR process loop also scales the resulting SAR magnitudes to the logarithmic radar rage equation 2.5. This result is outputted from the SAR loop and sent to the file save sequence.

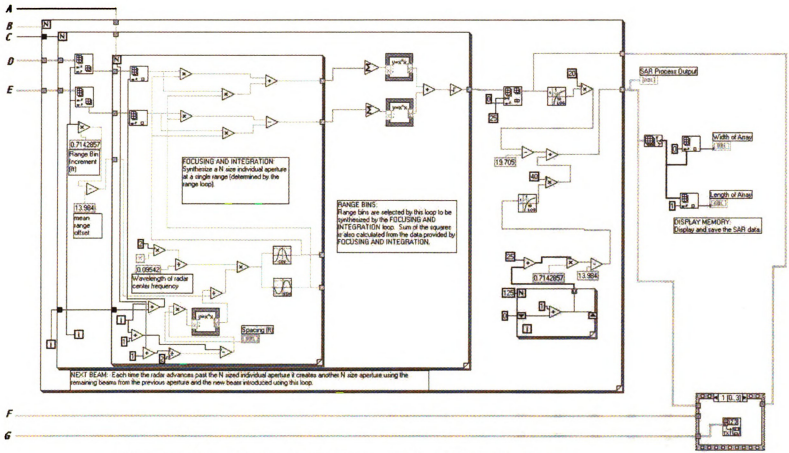

Figure 4.28b: Synthetic Aperture Radar VI block diagram, showing the SAR process loop and the file save sequence.

The file save sequence saves the data in a spreadsheet file from before and after the SAR process loop (see figure 4.28b). The file save sequence saves all of the data sequentially. First the absolute value of the real data from the data acquisition loop is saved. Next the data scaled to the radar range equation from the data acquisition loop is saved. Then the magnitude data from the SAR process loop is saved. Finally, the magnitude data scaled to the radar range equation from the SAR process loop is saved. The various data saved from the file save sequence is imported into Microsoft Excel, where it is plotted in 3 dimensions. The 3D plots show the radar image, produced before and after the SAR process. After all of the files are saved, the VI stops execution.

Chapter 5

Experimental Results

Four experiments were conducted using the unique FMCW radar solution. The tuning linearity was tested. The LO injection amplitude feeding MXR1 was tested. Two standard radar targets were designed and fabricated in order to test the radar system. The radar targets were then used to test the range linearity. And finally, the standard radar targets were used to test the system as a Synthetic Aperture Radar.

5.1 Tuning Linearity Experimental Results

The frequency of XCVR1 is voltage controlled. Ideally, the relation between voltage and frequency should be perfectly linear. However, the relationship between voltage and frequency is not. A plot of XCVR1 tuning voltage versus frequency relative to XCVR2 was plotted in figure 5.1.

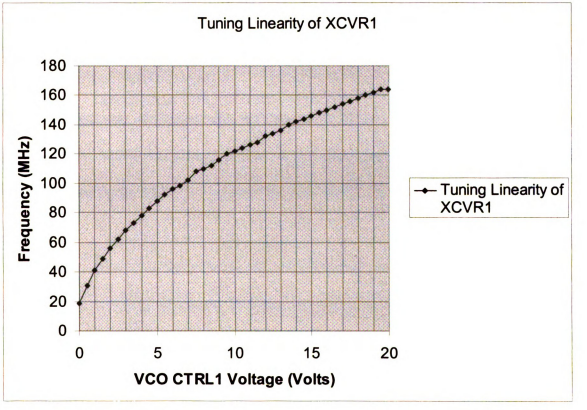

Figure 5.1: XCVR1 voltage versus frequency plot (relative to XCVR2).

In an FMCW radar system, tuning linearity is important. This was shown in equations 2.10 through 2.14. In the case of XCVR1, the most linear tuning range was found to be between 90 MHz and 160 MHz. This provides 70 MHz of transmit chirp bandwidth for the FMCW radar system. The corresponding tuning voltage for this frequency range is 5

V to 19 V. The amplitude of the ramp generator, and the offset potentiometer in the Modulation Amplifier were carefully set to accommodate the tuning voltage range of 5 V to 19 V. From these results, it was determined that the radar will perform the best if XCVR1 is modulated between the voltage range of 5 V to 19 V.

5.2 Local Oscillator Amplitude

The output of AMP2 is the LO drive signal for MXR1. AMP2 is setup as an adjustable limiter, where the output power limit is adjusted through a bias control potentiometer on the second stage of AMP2. The amplitude must be powerful enough and flat across the entire range of 90 MHz to 160 MHz (relative to XCVR2) in order for MXR1 to operate properly. The amplitude flatness depends on the coupling between XCVR1 and XCVR2, controlled by ATTN1. The amplitude flatness also depends on the bias control potentiometer inside of AMP2.

An experiment was conducted with ATTN1 set to 20 dB of coupling attenuation. The bias control of AMP2 was set to full bias. A plot of the amplitude on the output of AMP2 was made (see figure 5.2).

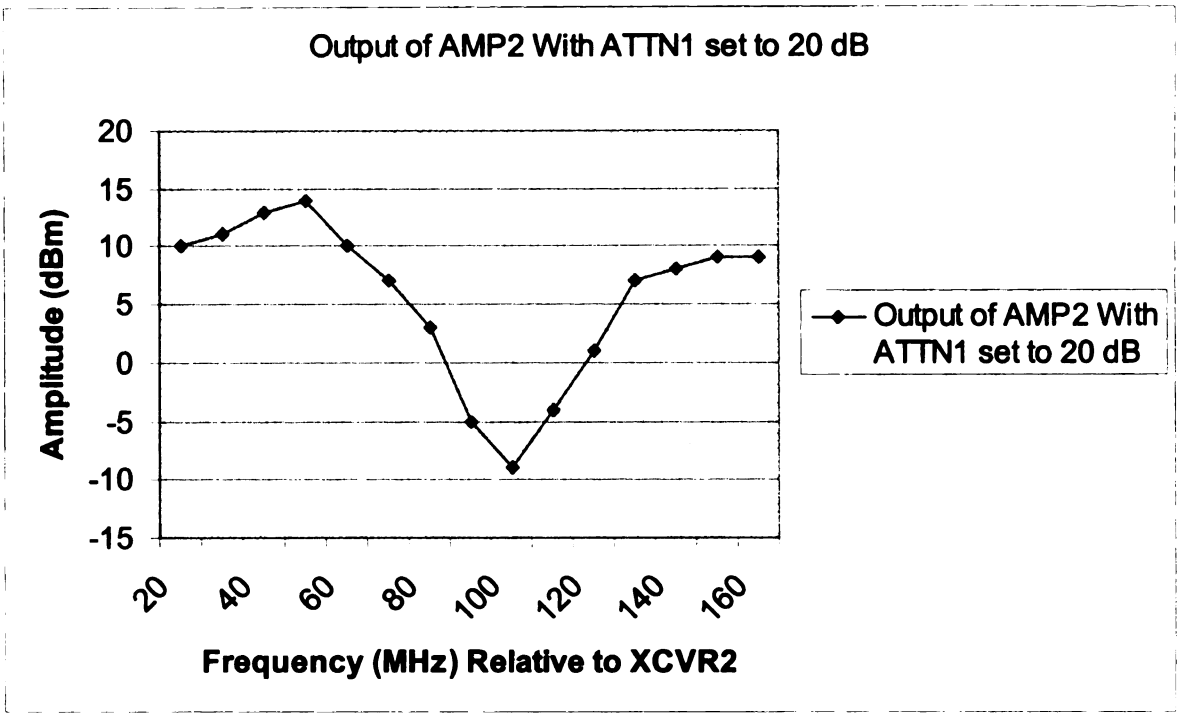

Figure 5.2: Power output of AMP2 versus frequency (relative to XCVR2), when ATTN1 is set to 20 dB.

The LO drive amplitude from the output of AMP2 was not flat over the tuning range of XCVR1. In order to overcome this problem, ATTN1 was set to 0 dB, maximum coupling. A second plot was made of the output power from AMP2, shown in figure 5.3.

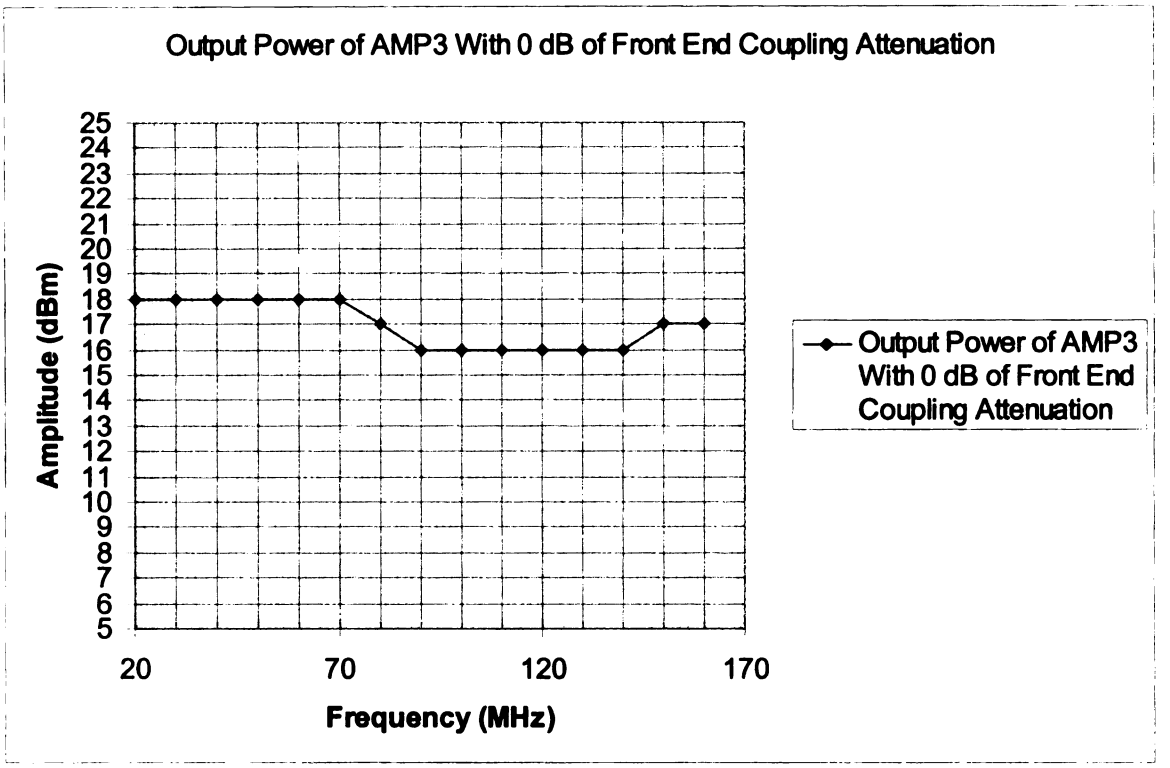

Figure 5.3: Power output of AMP2 versus frequency (relative to XCVR2), when ATTN1 is set to 0 dB.

When ATTN1 is set to 0 dB, the amplitude output of AMP2 is much more flat over the entire frequency range of XCVR1 (relative to XCVR2). It was decided that for optimum performance, ATTN1 will be set to 0 dB.

A further adjustment was made to the bias control on the second stage of AMP2. The bias control potentiometer inside of AMP2 was adjusted so that the maximum output power of AMP2 over the entire frequency range of XCVR1 will be limited to 8 dBm. It was found that these adjustments caused the LO drive level for MXR1 to be the most flat over the entire frequency range of XCVR1.

5.3 Standard Radar Targets

Two standard radar targets were created. Both of these targets are trihedral corner reflectors, with radar cross sections of 20 dBsm and 30 dBsm. The trihedral corner reflectors consist of three equally sized metal square plates, with dimension L (see figure 5.4).

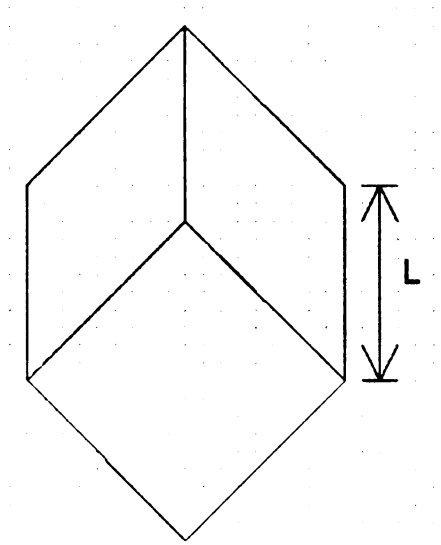

Figure 5.4: Trihedral corner reflector standard radar target.

The maximum radar cross section of a trihedral corner reflector target can be calculated using the equation [1]:

$$\sigma_{dB(\max)} = 10\log\left[\frac{12\pi L^4}{\lambda^2}\right] \tag{5.1}$$

Where: $\sigma_{dB(\max)}$ = maximum radar cross section in dBsm

L = length of the squares that make up the trihedral

From equation 5.1, the 20 dBsm target was found to have a length of 69.9 mm. The 30 dBsm target was found to have a length of 393.07 mm. Both targets were fabricated using 2 mm thick sheet aluminum, and are shown in figure 5.5.

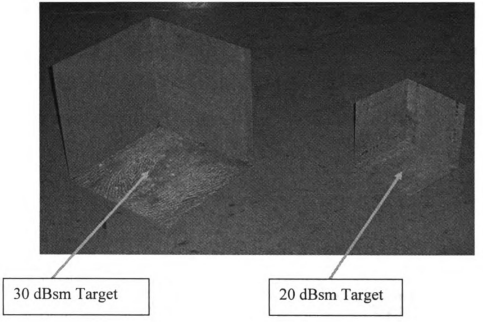

Figure 5.5: 20 dBsm and 30 dBsm trihedral corner reflector standard radar targets.

5.4 Single Beam Range to Target Experimental Results

A single beam range to target experiment was conducted to test the range linearity of the unique FMCW radar solution. In this experiment, the radar antennas were pointed down the length of large room. A measuring tape was laid down on the floor. A standard target mounted on a tripod was placed at various ranges from the radar antennas (see figures 5.6 and 5.7). The single range profile capture VI was then used to indicate and save the range to target measured by the radar system.

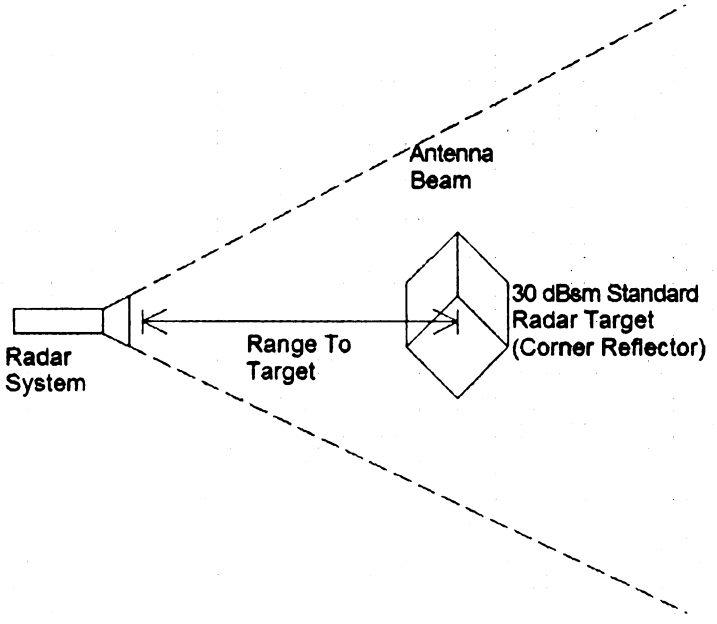

Figure 5.6: Single beam range to target experimental setup.

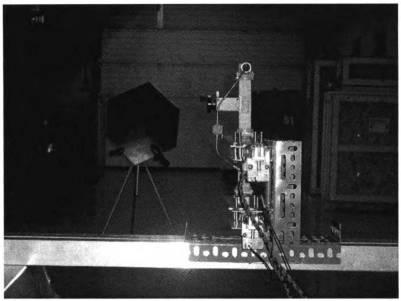

Figure 5.7: Picture of the experimental setup, where the 30 dBsm target is in the background, and the FMCW radar system is in the foreground.

The single range profile capture VI was set to sample 1000 samples at a rate of 200 KSPS. The ramp generator was set to produce a triangular waveform at a frequency of 100 Hz. From section 5.1, the FMCW radar system had a sweep bandwidth of 70 MHz. From this information, the resulting frequency range data is in the form of 14 Hz/foot for a round trip. This translates to 0.714 ft per x axis unit in the resulting range data displayed by the continuous operation and display VI. Range to target information displayed by the VI was noted and plotted. The difference between actual distance to target and the measured distance to target was also noted. The results are summarized in table 5.1.

Actual Distance (ft)	Measured Distance (ft)	Range Difference (ft)	Range Profile Plot
20	30.702	10.72	figure 5.8
25	38.199	13.199	figure 5.9
30	44.182	14.982	figure 5.10
35	50.337	15.337	figure 5.11
40	55.692	15.962	figure 5.12

Table 5.1: Single beam range to target experimental results summary.

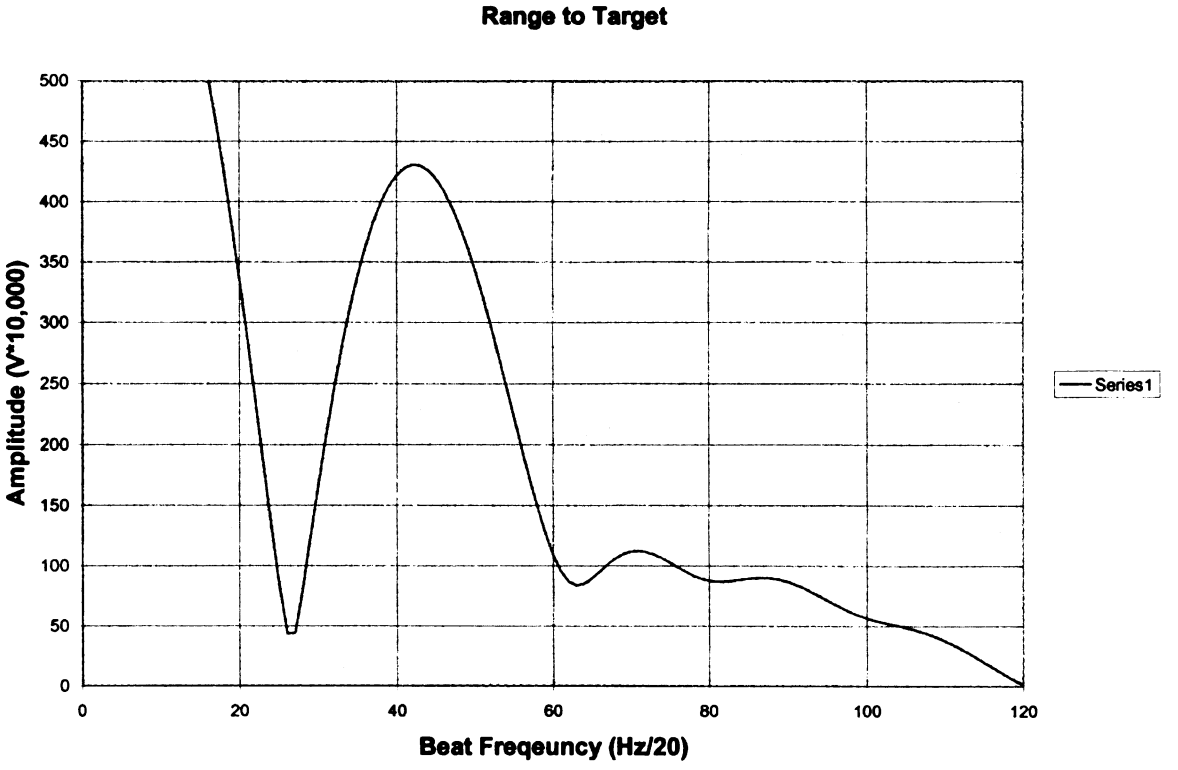

Figure 5.8: Range profile of 30 dBsm target at 20 ft.

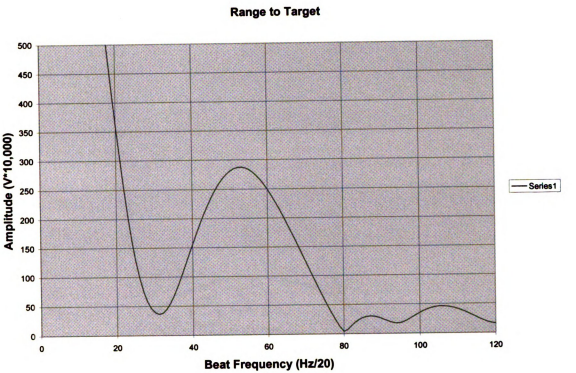

Figure 5.9: Range profile of 30 dBsm target at 25 ft.

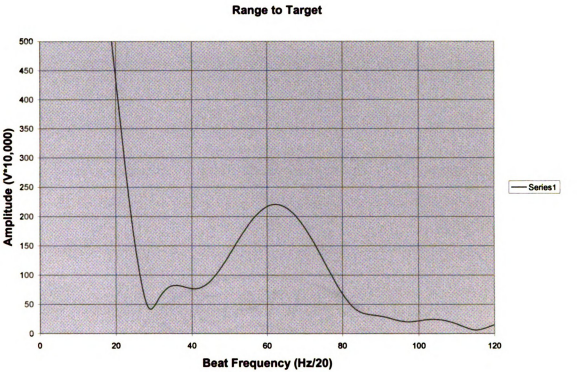

Figure 5.10: Range profile of 30 dBsm target at 30 ft.

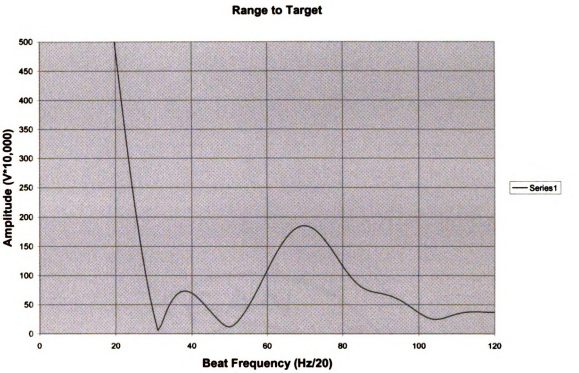

Figure 5.11: Range profile of 30 dBsm target at 35 ft.

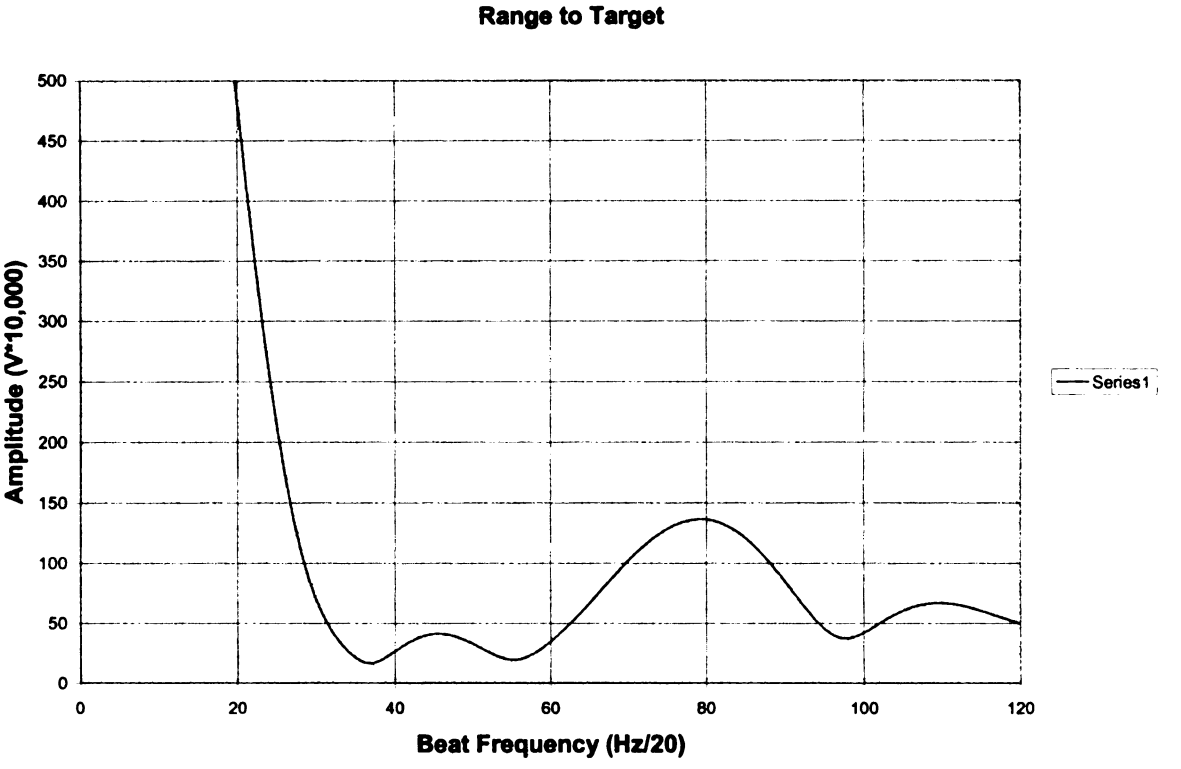

Figure 5.12: Range profile of 30 dBsm target at 40 ft.

From the results in table 5.1, and the magnitude range profiles in figures 5.8 through 5.12, differences in actual ranges to target and ranges measured by the radar are evident. These differences in range are due to the delay caused by the cables running from IF1 and IF2 to the IF Chassis. These range differences are also caused by the delays in the various amplifier components inside of the IF Chassis. Due to the range differences found, a mean range difference was calculated and found to be:

$$\text{Mean range difference} = \frac{\sum range\_differences}{5} = 13.984 \text{ ft} \qquad (5.2)$$

From this experiment, it was found that the mean range difference is 13.984 ft. This mean range difference was then factored into the Synthetic Aperture Radar VI, so that the aperture could be more accurately focused.

5.5 Synthetic Aperture Radar Experimental Results

From the previous sections, 5.1 through 5.4, the unique FMCW radar solution has been tested and adjusted for optimum performance, and standard targets were created to characterize performance. The final experiment in this study of the unique FMCW radar solution is the implementation of a Synthetic Aperture Radar imaging system.

For this experiment, the radar was setup in a large loading dock. The Front End was mounted on a 12 foot long aluminum track, supported by steel saw horses (see figure 5.13). The radar was moved down the track manually, and lined up with a measuring tape (see figure 5.14). Standard radar targets were placed down range from the system (see figure 5.15).

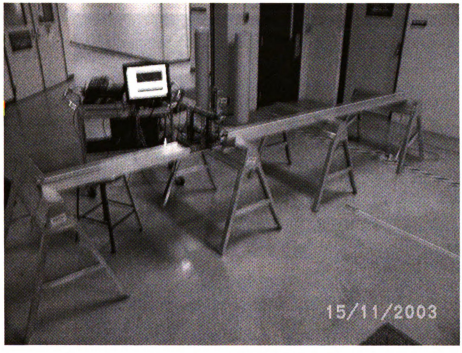

Figure 5.13: Synthetic Aperture Radar experimental setup.

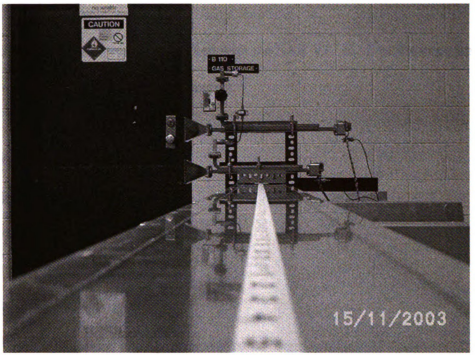

Figure 5.14: The Front End Assembly is manually pushed along the aluminum track and lined up with a measuring tape in order to create a SAR image.

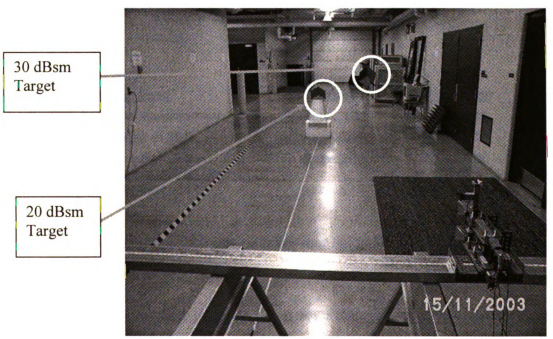

Figure 5.15: Both the 30 dBsm and 20 dBsm standard radar targets are placed down range from the SAR system.

Images of the standard targets were taken with the SAR VI. In all of the experiments, the SAR VI was set to the following parameters:

Number of Samples = 10,000

Sample Rate = 200 KSPS

FFT Sample Window Type = 3

Total Number of Beams = 138

Spacing (ft) = 0.08333

Number of Beams per Aperture = 32

Four different SAR images were taken using the standard targets. A list of the SAR images taken is shown in table 5.2.

Target Imaged	Data Before SAR Process	SAR Image
Nothing, base line measurement	figure 5.9	figure 5.16
30 dBsm target at 25 ft	figure 5.11	figure 5.17
20 dBsm target at 25 ft	figure 5.13	figure 5.18
20 dBsm target at 25 ft, and 30 dBsm target at 40 ft	figure 5.15	figure 5.19

Table 5.2: A list of the SAR images taken and their corresponding image plots.

The X axis units for the SAR images are in 0.714ft increments with a small range offset of 3.866 ft. The Y axis units are in 1 inch increments. The Z axis magnitude units are in

Volts*10K at 50 ohms. The radar system is located at the far right hand side of the image, facing the left hand side of the image.

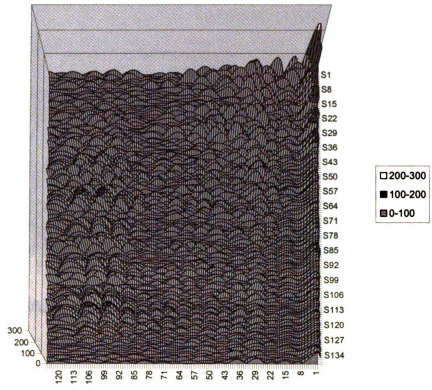

Figure 5.16: Base line measurement before SAR processing.

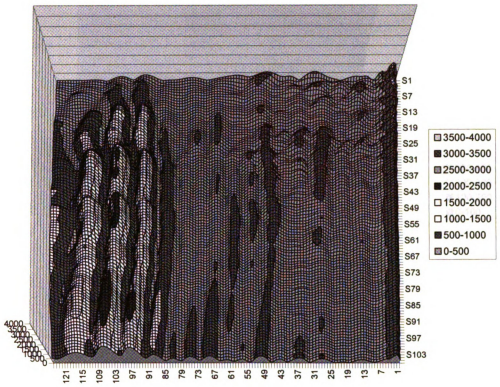

Figure 5.17: Base line measurement after SAR processing.

A base line measurement was taken with nothing present in front of the radar system except for the miscellaneous clutter in the location where the SAR data was captured. The base line measurement was taken as a reference, and for use in locating the ideal location to place standard targets. The before SAR processing data can be seen in figure 5.16, where the absolute value of the real range profile data is plotted. The data after SAR processing can be seen in figure 5.17. From the results shown in figure 5.17, it is apparent that the radar is picking up the various clutter located at the far end of the range (this clutter can be seen visually in figure 5.15).

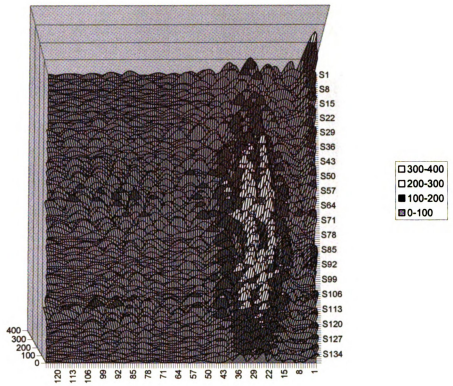

Figure 5.18: 30 dBsm target located at a distance of 25 ft before SAR processing.

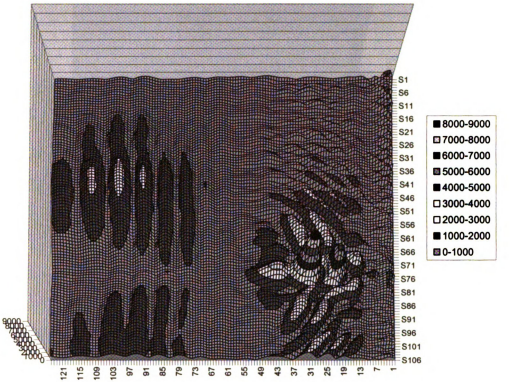

Figure 5.19: 30 dBsm target located at a distance of 25 ft after SAR processing.

A scan was taken of a 30 dBsm standard target at a range of 25 feet from the radar system. The data before SAR processing can be seen in figure 5.18, where the absolute value of the real range profile data is plotted. The data after SAR processing can be seen in figure 5.19. From these plots it is clear that the SAR process has successfully created a very strong image of the standard target at the correct location.

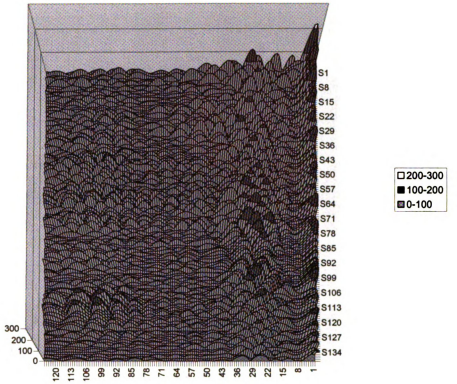

Figure 5.20: 20 dBsm target located at a distance of 25 ft before SAR processing.

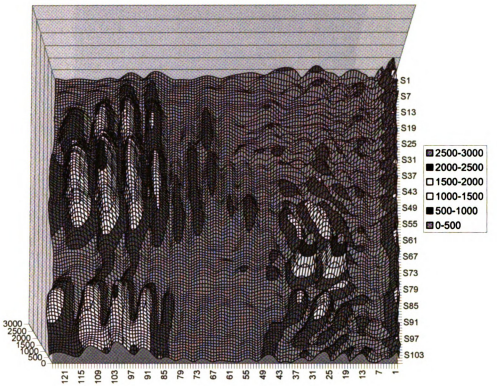

Figure 5.21: 20 dBsm target located at a distance of 25 ft after SAR processing.

A scan was taken of a 20 dBsm standard target at a range of 25 feet from the radar system. The data before SAR processing can be seen in figure 5.20, where the absolute value of the real range profile data is plotted. The data after SAR processing can be seen in figure 5.21. From these plots it is clear that the SAR process has successfully created a very strong image of the standard target at the correct location.

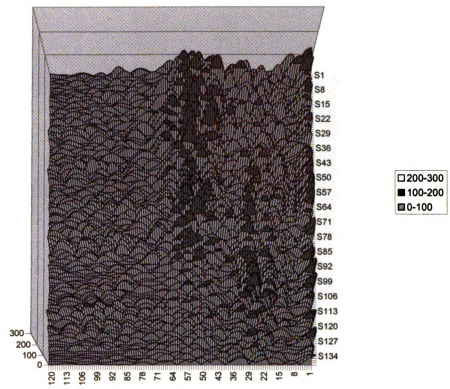

Figure 5.22: 20 dBsm target located at a distance of 25 ft, and a 30 dBsm target located at a distance of 40 ft before SAR processing.

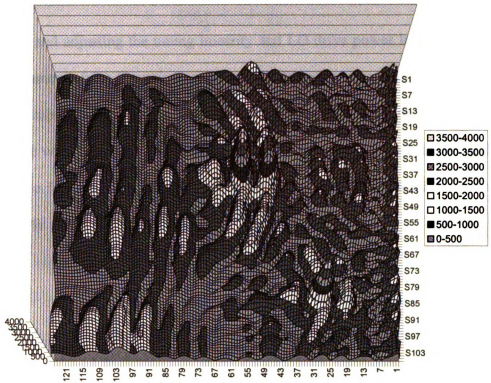

Figure 5.23: 20 dBsm target located at a distance of 25 ft, and a 30 dBsm target located at a distance of 40 ft after SAR processing.

And finally, a scan was taken of both targets, the 20 dBsm standard target at a range of 25 feet, and the 30 dBsm standard target at a range of 40 ft from the radar system. The data before SAR processing can be seen in figure 5.22, where the absolute value of the real range profile data is plotted. The data after SAR processing can be seen in figure 5.23. From these plots it is obvious that the SAR process has successfully created a very strong image of the standard targets, and is capable of differentiating between them downrange and cross range.

Summary:

After measuring and adjusting the tuning linearity and LO drive power level to MXR1, accurate measurements from the unique solution FMCW radar were made. The system was found to be capable of measuring range to target accurately, with some offset range. That offset range was then factored into the Synthetic Aperture Radar VI, allowing the system to acquire focused SAR images. In this section, the capabilities of the unique solution to FMCW radar have been shown.

Chapter 6

Conclusion

Continuous-wave radar is a proven design concept. The coherent design topology of traditional CW radar systems allows for simple implementation. CW radar is capable of providing the Doppler shift data of a moving target. When CW radar is frequency modulated, it is capable of providing range to target information. FMCW radar systems use expensive microwave coaxial components. However, it has been shown in the previous chapters that a lower cost alternative can be created with the use of two inexpensive microwave transceiver modules.

CW radar has been in use for many years. Wide spread use of FMCW radar occurred due to its practical application in radio altimeters. These FMCW radar altimeters have been in use since the mid 1930's. Similar radio altimeters are in use to date. Due to their application, very simple means of data acquisition and processing have been used in radio altimeters.

FMCW radar systems tend to use expensive coaxial microwave parts. Expensive parts are not a cost effective solution for high volume low power radar solutions. For this reason, a low cost FMCW radar solution was created. This low cost solution took

advantage of Gunn diode based microwave transceiver modules commonly found in motion sensors and radar speed guns.

This unique FMCW radar solution has been proven capable of determining range to target. More importantly, the unique solution has proven itself very effective in the advanced radar application of Synthetic Aperture Radar. Detailed images were created of standard targets at various ranges, using data from the unique solution to FMCW radar.

Future work on this unique solution to FMCW radar should include creating a method for increasing the transmit chirp bandwidth, increasing transmit power, automating the sliding track used to create SAR images, and testing the ability to use multiple sensors in close proximity. One way of increasing the chirp bandwidth would be to phase lock XCVR1 to a highly accurate low frequency chirp reference. An increased chirp bandwidth would cause an increase in range resolution. Increasing the transmit power would in effect cause an increase in system sensitivity. Since the noise figure of the transceiver modules is unchangeable, an increase in transmit power is required in order for the system to detect smaller radar targets. Automating the metal track used to create SAR images would minimized phase errors caused by moving the radar system manually. Testing multiple radar units in close proximity must be done to determine the feasibility of deploying multiple inexpensive radar sensors. This test would be necessary for determining to what extent the radar sensors interfere with each other, and if it is possible to prevent such interferences.

Test results show that this unique solution to FMCW radar has great potential for more advanced applications. The use of inexpensive radar solutions will become increasingly important in the near future for use in high volume applications where a reliable range to target sensor is needed. It is the conclusion of the author that this unique solution to frequency-modulated continuous-wave radar is a practical low cost alternative to previous FMCW radar designs.

References

[1] M. I. Skolnic, "Radar Handbook." New York: McGraw-Hill, 1970.

[2] J. L. Eaves, and E. K. Ready, "Principles of Modern Radar." New York: Van Nostrand Reinhold Company, 1987.

[3] M. P. G. Capelli, "Radio Altimeter," IRE Transactions on Aeronautical and Navigational Electronics, vol. 1, pp. 3-7; June 1954.

[4] F. T. Wimberly and J. F. Lane, "The AN/APN-22 Radio Altimeter," IRE Transactions on Aeronautical and Navigational Engineering, vol. 1, pp. 8-14; June 1954.

[5] A. Black, K. E. Buecks, and A. H. Heaton, "Improved Radio Altimeter," Wireless World, vol. 60, pp. 138-140; March 1954.

[6] G. W. Stimson, "Introduction to Airborne Radar." El Segundo, California: Hughes Aircraft Company, 1983.

[7] "The ARRL Handbook, 71st Edition." Newington, Connecticut: The American Radio Relay League, Inc, 1994.

[8] C. A. Balanis, "Antenna Theory, Analysis and Design, 2nd Edition." New York: John Wiley & Sons Inc, 1997.

[9] J. J. Carr, "Secrets of RF Circuit Design, 2nd Edition." New York: McGraw-Hill, Inc, 1997.

[10] S. E. Craig, W. Fishbein, and O. E. Rittenbach, "Continuous-Wave Radar With High Range Resolution and Unambiguous Velocity Determination," IRE Transactions on Military Electronics, vol. MIL-6, no. 2, April 1962, pp. 153-161.

[11] J. D. Kraus, "Antennas, 2nd Edition." New York: McGraw-Hill, Inc, 1988.

[12] U. L. Rohde, J. Whitaker, and T. T. Bucher, "Communications Receivers, 2nd Edition." New York: McGraw Hill, Inc, 1997.

[13] W. K. Saunders, "Post-War Developments in Continuous-Wave and Frequency-Modulated Radar," IRE Transactions in Aerospace and Navigational Electronics, vol. ANE-8, no. 1, March 1961, pp. 7-19.

[14] P. Vizmuller, "RF Design Guide, Systems, Circuits, and Equations." Boston: Artech House, 1995.

[15] R. E. Ziemer, and W. H. Tranter, " Principles of Communications, Systems, Modulation, and Noise, 4th Edition." New York: John Wiley & Sons, Inc., 1995.